Energy Conversion and Management 96 (2015) 208–227

Contents lists available at ScienceDirect

Energy Conversion and Management

journal homepage: www.elsevier.com/locate/enconman

Performance analysis of proposed hybrid air conditioning and humidification–dehumidification systems for energy saving and water production in hot and dry climatic regions

S.A. Nada [a,*], H.F. Elattar [a], A. Fouda [b]

[a] Department of Mechanical Engineering, Benha Faculty of Engineering, Benha University, Benha, 13511 Qalyubia, Egypt
[b] Department of Mechanical Power Engineering, Faculty of Engineering, Mansoura University, 35516 El-Mansoura, Egypt

ARTICLE INFO

Article history:
Received 13 December 2014
Accepted 26 February 2015

Keywords:
Water desalination
Air conditioning
Humidification–dehumidification
Energy saving
Energy recovery

ABSTRACT

Performance of integrative air-conditioning (A/C) and humidification–dehumidification desalination systems proposed for hot and dry climatic regions is theoretically investigated. The proposed systems aim to energy saving and systems utilization in fresh water production. Four systems with evaporative cooler and heat recovery units located at different locations are proposed, analyzed and evaluated at different operating parameters (fresh air ratio, supply air temperature and outside air wet bulb temperature). Other two basic systems are used as reference systems in proposed systems assessment. Fresh water production rate, A/C cooling capacity, A/C electrical power consumption, saving in power consumptions and total cost saving (TCS) parameters are used for systems evaluations and comparisons. The results show that (i) the fresh water production rates of the proposed systems increase with increasing fresh air ratio, supply air temperature and outdoor wet bulb temperature, (ii) powers saving of the proposed systems increase with increasing fresh air ratio and supply air temperature and decreasing of the outdoor air wet bulb temperature, (iii) locating the evaporative cooling after the fresh air mixing remarkably increases water production rate, and (vi) incorporating heat recovery in the air conditioning systems with evaporative cooling may adversely affect both of the water production rate and the total cost saving of the system. Comparison study has been presented to identify systems configurations that have the highest fresh water production rate, highest power saving and highest total cost saving. Numerical correlations for fresh water production rate and total system energy consumption are developed and presented in terms of the controlling parameters.

© 2015 Elsevier Ltd. All rights reserved.

1. Introduction

World population growth and the increase of industrial and human activities have led to excessive needs of air conditioning and potable/drinkable water, especially in hot and dry climatic regions. Recently, hybrid air conditioning and water desalination systems using humidification–dehumidification technique driven by mechanical vapor compression (MVC) are used for energy saving. MVC desalination was one of the most efficient thermal distillation processes for its compactness and suitability for small and large potable unit. Faisal et al. [1] developed mathematical models and performed a comparison for four different types of single-effect evaporator desalination systems (thermal, mechanical, absorption, and adsorption vapor compression heat pumps). Siqueiros and Holland [2] carried out a review of the experimental works on water purification driven by heat pump. Slesarenko [3] suggested incorporating heat pumps as a source of heat energy for seawater desalination plants. Two plants were proposed; one operated with compression heat pump using R12 and the other operated with steam and water cycle. Al-Ansari et al. [4] modeled and analyzed a single effect evaporation desalination process combined with adsorption heat pump (ADVC) in terms of designed and operational system parameters. Aly et al. [5] described and studied theoretically and experimentally the performance of the mechanical vapor compression (MVC) desalination system. Hawlader et al. [6] described a novel solar assisted heat pump desalination system. The effects of feed water temperature and flashing have been investigated. The study revealed that a good fresh water production rate can be obtained from the system. Heat pumps using agent R12 or water and vapor to be used as a source of heat energy for seawater desalination were introduced by Jinzeng and Huang [7].

* Corresponding author. Mobile: +20 1066611381.
E-mail address: samehnadar@yahoo.com (S.A. Nada).

http://dx.doi.org/10.1016/j.enconman.2015.02.082
0196-8904/© 2015 Elsevier Ltd. All rights reserved.

Nomenclature

$\dot{E}$	total electric power, kW
TCS	total cost saving
h_{fg}	latent heat of evaporation of water, kJ/kg
i	specific enthalpy, kJ/kg
$\dot{m}$	mass flow rate, kg/s
$\dot{m}_{steam}$	steam mass flow rate, kg/s
$\dot{Q}$	refrigeration capacity, kW
R	water system recovery
RSHF	room sensible heat factor
T	temperature, °C
TR	Tone of refrigeration
W	air specific humidity, $kg_{water}/kg_{dry\ air}$
W_c	compressor power, kW

Greek symbols

η_h	humidifier efficiency
ε	effectiveness of heat recovery

Subscript

A	air
BS	basic systems
Cc	cooling coil
Db	dry bulb
E	evaporator
evc	evaporative cooler
feed	feed water
H	humidifier
I	inlet
Min	minimum
Max	maximum
O	outlet
R	room
RH	relative humidity
PS	proposed systems
S	conditioned space supply state
W	water
Wb	wet bulb

Yuan et al. [8] presented an integrative unit for air-conditioning and desalination driven by vapor compression heat pump on basis of direct humidification–dehumidification process. The performance of a new type of a humidification–dehumidification desalination unit driven by mechanical vapor compression heat pump using mathematical model to study the flow and heat and mass transfer inside the humidifier was analyzed by Gao et al. [9]. Wu et al. [10] analyzed theoretically the heat and mass transfer between air and water film in the direct evaporative cooler. An open air–vapor compression refrigeration system for both air-conditioning and desalination on ship cooled by seawater was presented by Houa et al. [11]. The heat and mass transfer between water and air in a direct evaporative cooler was developed by Wu et al. [12] using numerical model with treating the mass of evaporated water as a mass source of air flow, and the latent heat of water evaporation as a heat source in the energy equation. Performance study of a combined heat pump (HP) with a dehumidification process to produce fresh water from the atmospheric air was analyzed by Habeebullah [13]. Nada et al. [14] experimentally investigated the performance of a hybrid humidification–dehumidification water desalination and air conditioning system using vapor compression refrigeration cycle. Attia [15] introduced a new proposed system for freeze water desalination using auto reversed R-22 vapor compression heat pump, the system depends on optimization of utilizing the heat flow of the heat pump system to increase the whole system efficiency. Rane and Padiya [16] discussed a patented layer freezing based technology which was scalable and coupled with a heat pump to switch freezes water from seawater in the evaporator and melts the ice in the subsequent phase when it serves as a condenser. Jain and Hindoliya [17] presented performance analysis of two new evaporative cooling pad materials namely coconut fibers and palash fibers and compared with that of aspen and khus pads which are commonly made now-a-days. Malli et al. [18] studied experimentally the thermal performance of two types of cellulosic evaporative cooling pads which were made from corrugated papers. Mehrgoo, and Amidpour [19] used the constructal theory for conceptual design of a humidification dehumidification (HD) desalination unit and they showed that the main design features of a direct contact HD desalination process can be determined based on the method of the constructal design. Shatat et al. [20] developed a mathematical model to describe the affordable small scale solar water desalination plant using the psychometric humidification and dehumidification process coupled with an evacuated tube solar collector.

Performance limits of zero and single extraction humidification–dehumidification desalination systems was investigated theoretically by McGovern et al. [21]. The investigation was done by considering heat and mass exchangers to be sufficiently large to provide zero pinch point temperature and concentration differences within the humidifier and dehumidifier. Shen et al. [22] presented a comprehensive analysis of a single-effect of mechanical vapor compression (MVC) desalination system using water injected twin screw compressors. The operational characteristics of the twin screw compressor including inlet volume flow rate, compressor pressure ratio, and mass fraction of injected water were investigated. Theoretical study of a simple solar still coupled to a compression heat pump using mass and heat balance was presented by Halima et al. [23].

Kang et al. [24] developed a mathematical model to investigate the performance of a two-stage multi-effect desalination system based on humidification–dehumidification process with variation of the control parameters. Younes et al. [25] presented new humidification–dehumidification process desalination technology named "Humidification Compression (HC)" which has some advantages (such as: high energy performance, high recovery flow rate, energy recovery) in comparison with other similar methods. Aybar [26] presented mathematical modeling to study the operation characteristics of a low-temperature mechanical vapor compression desalination system. The compressor work and the mass flow rate of the distilled water were investigated against the evaporation side pressure, the condensation side pressure, and the water inlet temperature. Zhang et al. [27] proposed a novel air dehumidification system, namely, mechanical dehumidification with membrane-based total heat exchanger using thermodynamic modeling. The annual primary energy consumptions for the system through hour-by-hour analysis was presented and discussed. Bahar et al. [28] performed experimental work on a mechanical vapor compression desalination system (MVC). The performance of the system was evaluated under different values of brine recirculation rate and compressor speed. Ettouney et al. [29] proposed

a mathematical model to analyze the single-effect mechanical vapor-compression (MVC) desalination systems as a function of the system design and operating parameters.

Al-Enezi et al. [30] measured and analyzed the performance characteristics of the humidification dehumidification desalination system at low operating temperatures. The highest water production rates were obtained at high hot water temperature, low cooling water temperature, high air flow rate and low hot water flow rate. Nafey et al. [31] studied theoretically and experimentally small unit solar water desalination system using flashing process. A mathematical model was developed to calculate the productivity of the system under different operating conditions. Mohamed and El-Minshawy [32] carried out theoretical work to evaluate the performance of sea water humidification–dehumidification desalination system powered by solar energy. The theoretical simulation model was developed and a comparison study had been presented to show the effect of the different parameters on the system performance and its productivity. Ghazal et al. [33] carried out experimental prototype to improve the performance of solar HDD systems. The solar air heater, solar water heater and the evaporator of the traditional HDD systems were replaced with compact system designs. Yıldırım and Solmus [34] investigated theoretically the performance of a solar powered humidification–dehumidification desalination system for various system operating and design parameters under climatological conditions of Antalya, Turkey. Clean water production is positively affected by the increasing air mass flow rate and feed water mass flow rate.

According to authors' review there is a shortage in the utilization of a large capacity air conditioning system of hot and dry climatic regions driven by chillers to produce potable/drinkable water from raw water (seawater, brackish water, well water, etc.) and at the same time reduce the air conditioning system power consumptions by incorporating evaporative coolers and heat recovery units to the air conditioning systems. Therefore, the present work aims to (i) proposes different configurations of large capacity hybrid air conditioning systems with heat recovery and humidification-dehumidification water purification systems for the purpose of economically production of fresh water and considerable energy saving of the air conditioning system, (ii) studying, the effects of the different system operating parameters (fresh air ratio, space supply air temperature and wet bulb temperature of outside air) on the fresh water production rate, saving in the energy required to operate the air condition systems, and (iii) comparisons of the different proposed systems for selecting the optimum systems at the different operating conditions based on the total cost saving due to air condition energy saving and fresh water production.

2. Systems description

Six systems are studied; two basic systems: system A and system B with and without heat recovery unit and other two proposed modified systems of each of the two basic system using evaporative cooling at two different locations of the air conditioning systems. All systems are considered to serve a building having 1000 TR conditioned space cooling load (this is a considered value and the study is valid for any cooling load) with a room sensible heat factor (RSHF) = 0.9. The air conditioning systems are considered to be powered by a water cooled chillers which are suitable for dry areas. Figs. 1 and 2 show schematic and the Psychrometric diagrams of the two basic air conditioning systems; system A and systems B, respectively. The two basic systems are used as reference systems in evaluation and comparison of the proposed modified four systems. System A consists of conditioned space, cooling and dehumidifying cooling coil, water cooled chiller unit, steam humidifier, and system-B consists of the same components of system A in addition to heat recovery unit. The steam humidifier is normally used in dry climatic regions to maintain the required relative humidity inside the condition spaces within thermal comfort values. Air at ambient condition (O) is mixed with returned air (R) as in system A or cooled to (O′) in heat recovery before mixing with returned air as in system-B to obtain air at state (M). The mixed air is then passes through steam humidifier where it is humidified to attain state (M′). The amount of steam injected in the humidifier is controlled to maintain the required relative humidity inside the conditioned space. The humidified air then passes through the cooling coil, where it is sensible cooled. Figs. 1b & 2b illustrate the psychrometric cycles at 25% and 100% fresh air ratio, for system-A and system-B, respectively. The psychrometric cycles are O-R-M-M'-S-R and O-M″-S-R for system-A at 25% and 100% fresh air ratio, respectively and O-O′-R-M-M′-S-R and O-O′-M″-S-R for system-B at 25% and 100% fresh air ratio, respectively. As shown on the charts, by increasing the fresh air ratio, the line MM′ moves towards the line OM″ (System-A) and the line O′M″ (System-B) until it completely coincides on it at 100% fresh air.

Figs. 3–6 illustrate the schematic and psychometric diagrams of the four proposed modified systems; system C, D, E, and F by using evaporative cooler in system-A and system-B at two different location; upstream and downstream the mixing the fresh air with the return air. In systems C & D, an evaporative cooler is placed before the mixing process in system-A and system-B, respectively but in systems E & F, the evaporative cooler is placed after the mixing process in system-A and system-B, respectively. In the four proposed systems, the steam humidifier was eliminated as its function is carried out with the evaporative coolers. In system C, air at the ambient condition (O) is cooled and humidified by sea water humidifier to (O′), then mixed with returned air (R). The mixing air is then passes through the cooling and dehumidifying coil where the air is cooled and dehumidified and the water vapor condenses on the dehumidifier surface producing fresh water. Finally the cooled and dehumidified air is supplied to the conditioned space at (S) to carry up the building cooling load. In system D the fresh air at (O) is firstly cooled to (O′) in heat recovery and then passes through the same cycle of System-C. In systems E and F the fresh air at condition (O) or (O′), respectively is firstly mixed with returned air (R) before humidifying it in the evaporative cooler and then passes through the same cycle of System-C and D, respectively. Figs. 3b & 4b illustrate the psychometric cycles at 25% and 100% fresh air ratio for systems-C and D, respectively. For system C, the psychometric cycles are O-O′-R-M-S-R at 25% fresh air and O-O′-S-R at 100% fresh air and for system D the psychometric cycles are O-O′-O″-R-M-S-R at 25% fresh air and O-O′-O″-S-R at 100% fresh air, respectively. Figs. 5b & 6b illustrate the psychometric cycles at 25% and 100% fresh air ratio for systems-E and F, respectively. For system-E, the psychometric cycles are O-R-M-M′-S-R at 25% fresh air and O-M″-S-R at 100% fresh air and for system-F the psychometric cycles are O-O′-R-M-M′-S-R at 25% fresh air and O-O′-M″-S-R at 100 % fresh air, respectively. As shown on Figs. 3b–6b for systems C, D, E and F, point M moves away from point R as the fresh air percentage increase until it coincides on points O′, O″, O and O' in systems-C, D, E and F, respectively.

3. Thermodynamic analysis and mathematical modeling

The governing equations based on energy and mass balance are derived for each of the system components and solved numerically by developing mathematical model to simulate the systems in equations using EES (Engineering Equation Solver, commercial version 6.883-3D) software. The model proposed is based on the following assumptions:

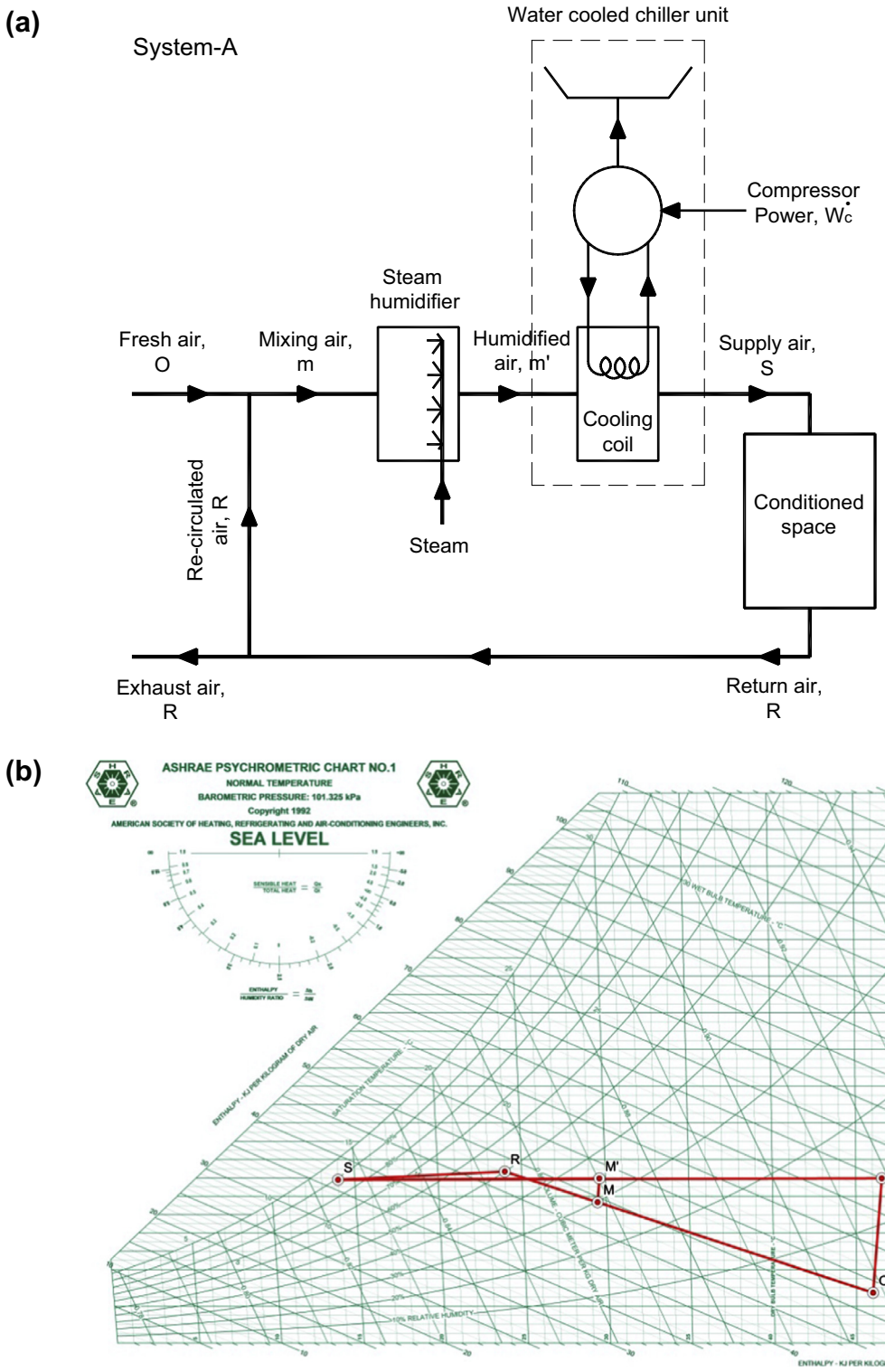

Fig. 1. Schematic and psychometric diagrams of basic system-A: (a) schematic, (b) psychromitric chart.

- Air to air heat recovery and evaporative cooler efficiencies are taken as 60% and 95%, respectively as per typical values of suppliers [10,12,35].
- There are no air and water leakages from the system components; humidifier, heat recovery, humidifier, cooling and dehumidifying coils and air ducting system.
- The dry-bulb temperature of ambient air is 46 °C as a typical design value for hot climatic zones (for example Golf cities).
- Coefficient of performance of water cooled condenser chiller system = 6 as per typical value of suppliers [36].
- Inside design conditions of the conditioned space is constant during the study and equals $T_{db,R}$ = 24 °C & RH = 50% for thermal comfort.
- RSHF = 0.9.
- The circulating pump power of the evaporative cooler is negligible as compared to the power of the air conditioning system.

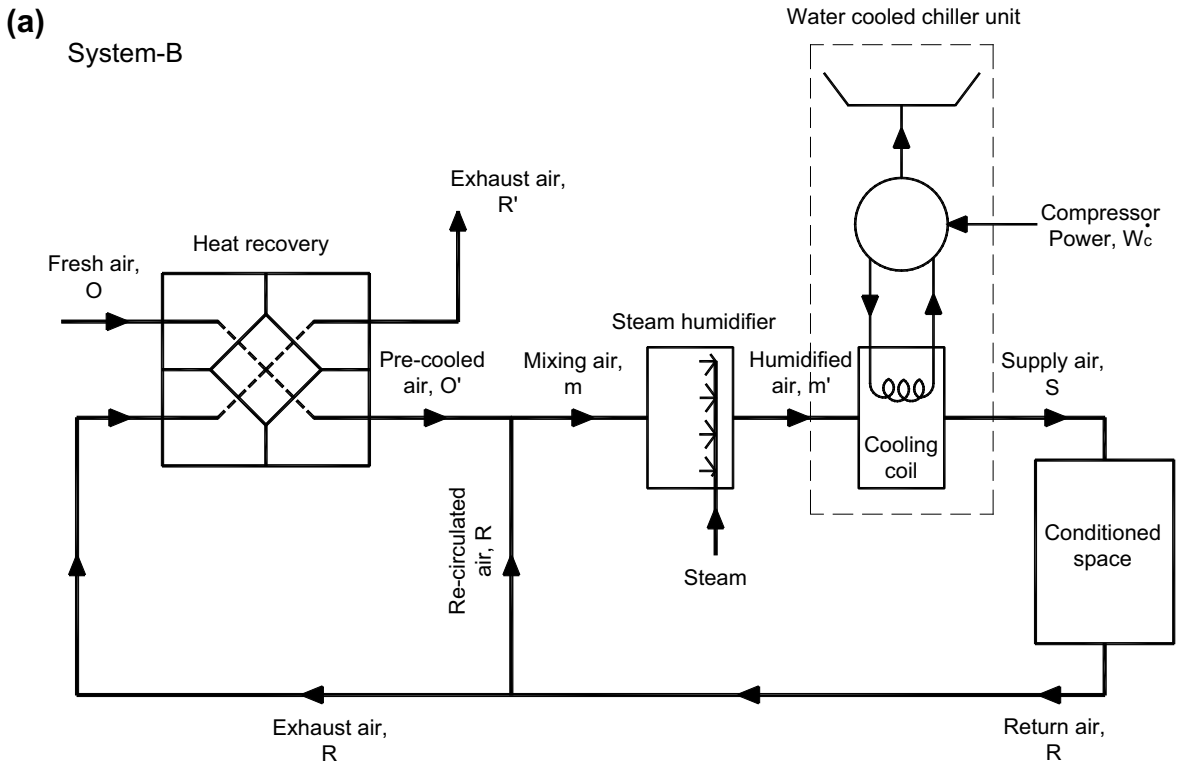

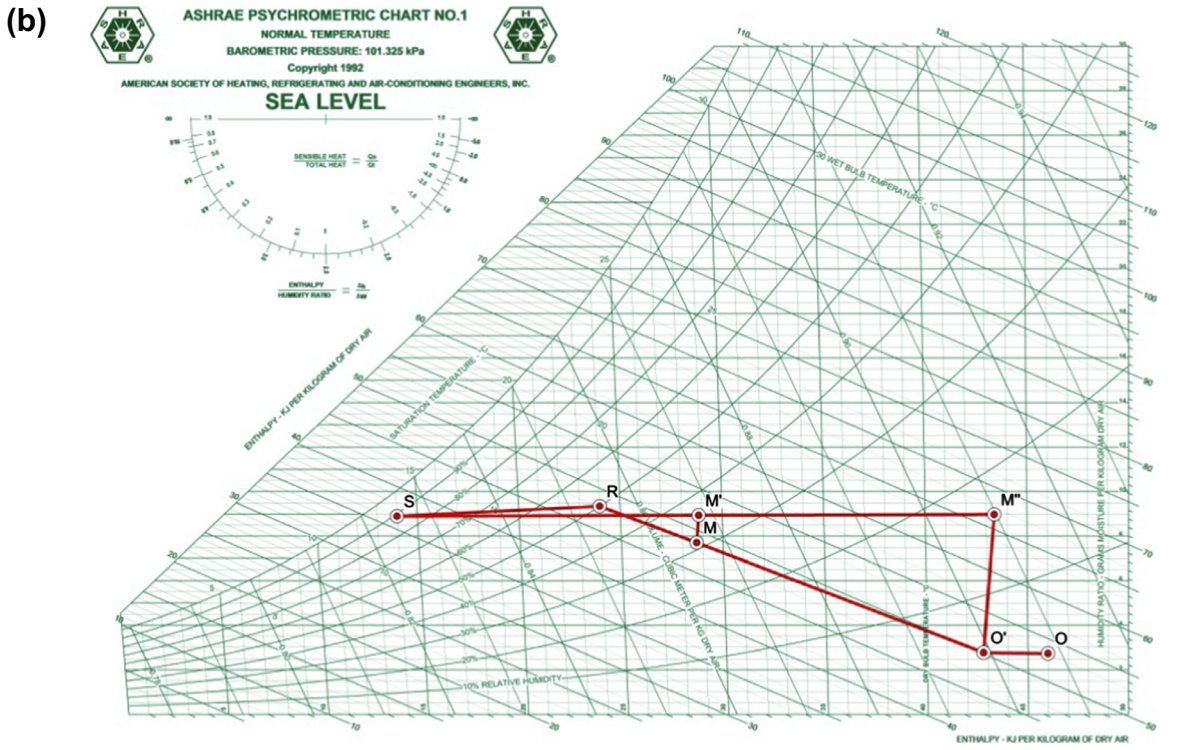

Fig. 2. Schematic and psychometric diagrams of basic system-B: (a) schematic, (b) psychromitric chart.

- The properties and type of the raw water (sea water, brackish water, well water …etc) do not affect the thermodynamics analysis (subject of the study) of humidification process as the raw water is at ambient temperature and the humidification process in the evaporative cooler is a constant wet bulb temperature process (adiabatic evaporation process). The only controlling parameters of this process are the properties of the air.
- Fresh water obtained from the cooling coil is obtained at the cooling coil apparatus temperature.
- The salt concentration in the formed vapor is zero [21], therefore distillate fresh water needs chemical treatment (see Figs. 3a–6a) to be potable water salinity (500 ppm according to the WHO (World Health Organization) recommended value).

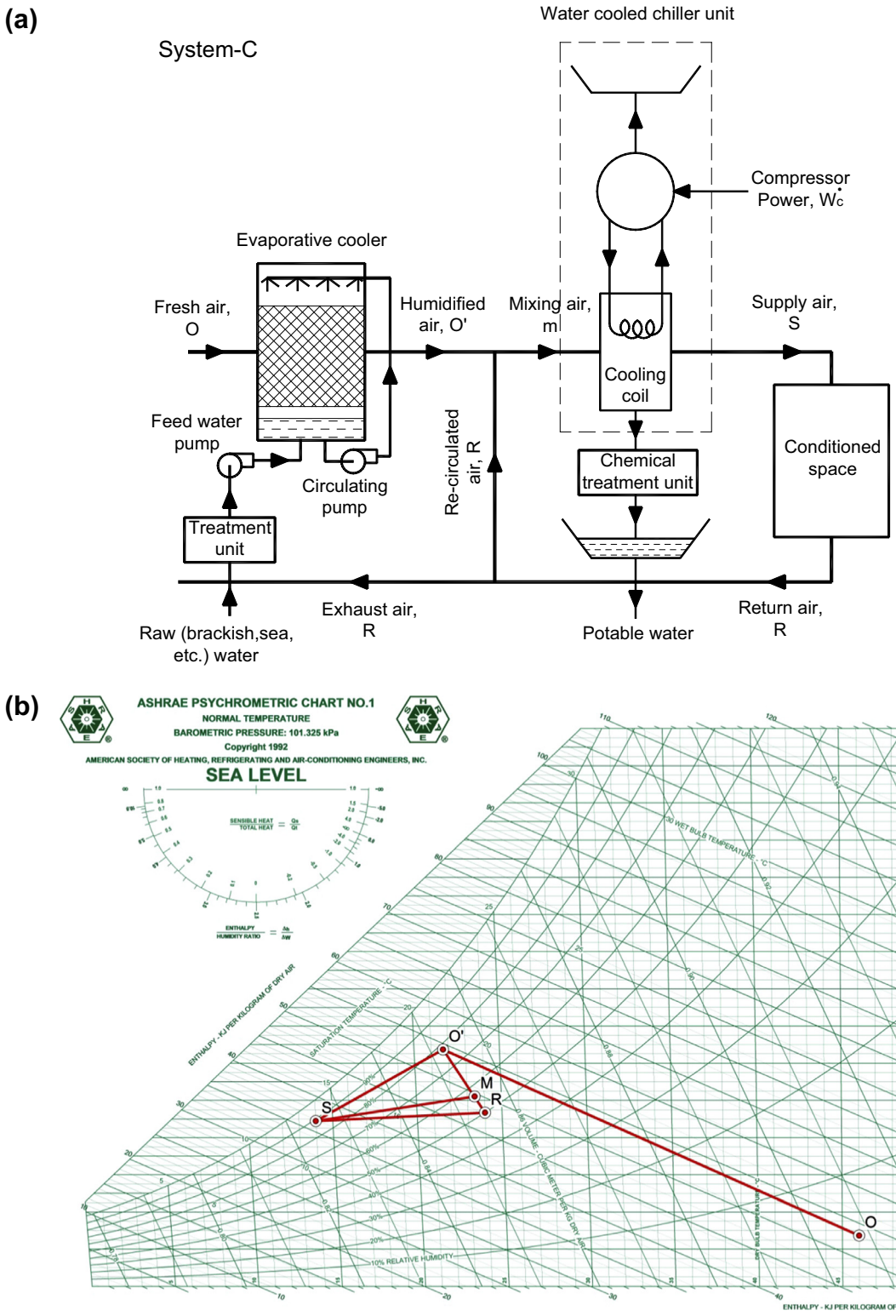

Fig. 3. Schematic and psychometric diagrams of proposed system-C: (a) schematic, (b) psychometric chart.

- Specific auxiliary work (the ratio of the auxiliary electricity consumed by blowers and pumps used for air and water circulation per unit amount of water production is a small (about 0.029 kW h per cubic meter desalinated water [37]) and negligible with respect to the power of the air conditioning system.
- The effect of the water characteristics (sea water or brackish water) on the humidifier performance due to scaling was considered to be avoided by using regular chemical washing for evaporative cooling and self-cleaning. Therefore in the present analytical work the humidification efficiency in the evaporator cooler is assumed to be fixed (95%) independent on the water characteristics.

Fresh water production rate, supplied air flow rate to conditioned space, cooling coil capacities (total and latent) and injected steam flow rates (for basic systems-A and B) are calculated from

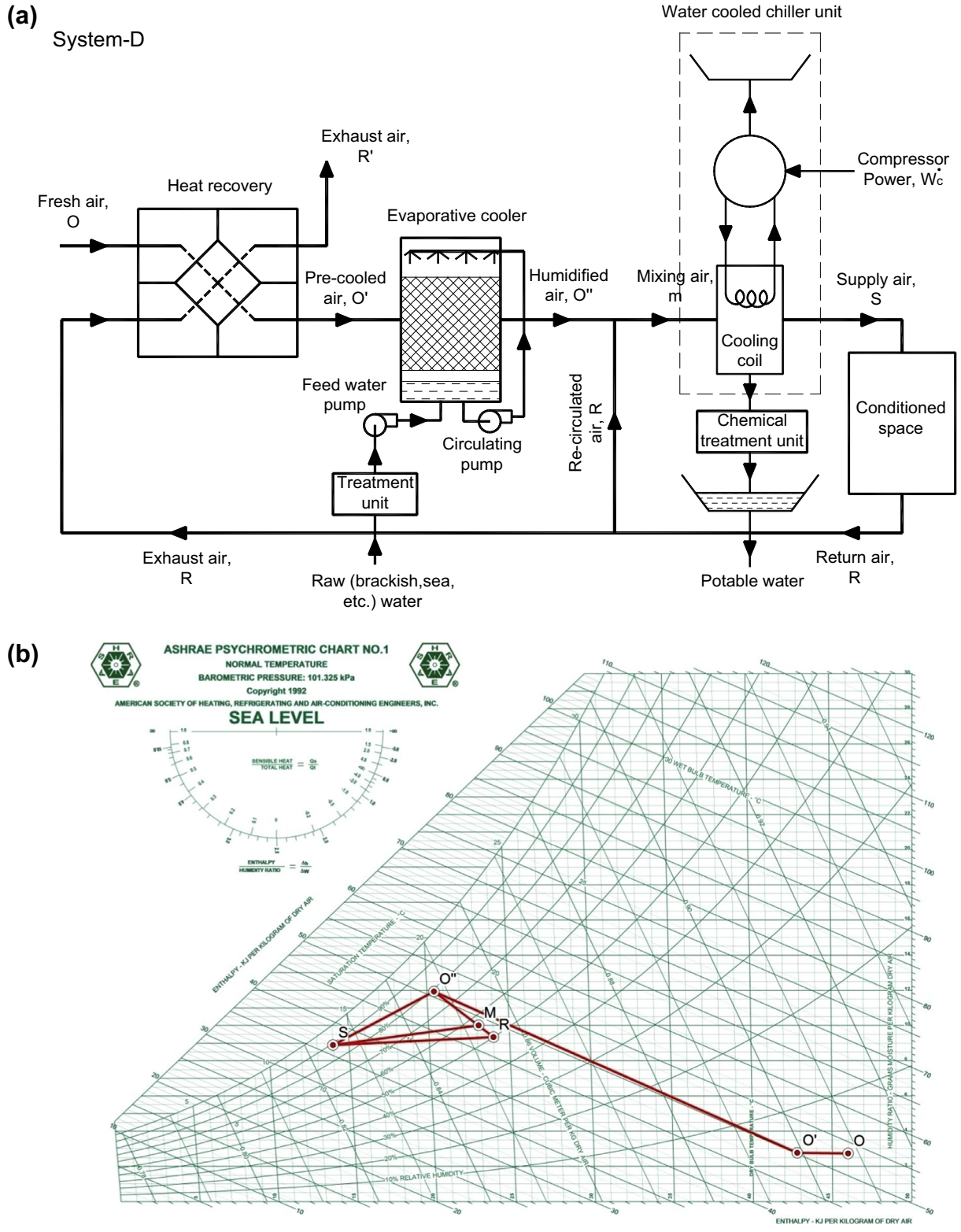

Fig. 4. Schematic and psychometric diagrams of proposed system-D: (a) schematic, (b) psychometric chart.

mass balance and heat balance of the air conditioning system equipment (heat recovery, mixing section, evaporative cooler, steam humidifier, cooling coil, and conditioned space) and the air properties of the different states points of the psychrometric cycles shown in Figs. 1b–6b, as follows:

$$\dot{m}_w = \dot{m}_a(w_{a,i,e} - w_{a,o,e}) \tag{1}$$

$$\dot{m}_a = \frac{\dot{Q}_R}{(i_{a,R} - i_{a,S})} \tag{2}$$

$$\dot{Q}_{c.c} = \dot{m}_a(i_{a,i,e} - i_{a,o,e}) \tag{3}$$

$$\dot{m}_{steam} = \dot{m}_a(w_{a,o,h} - w_{a,i,h}) \tag{4}$$

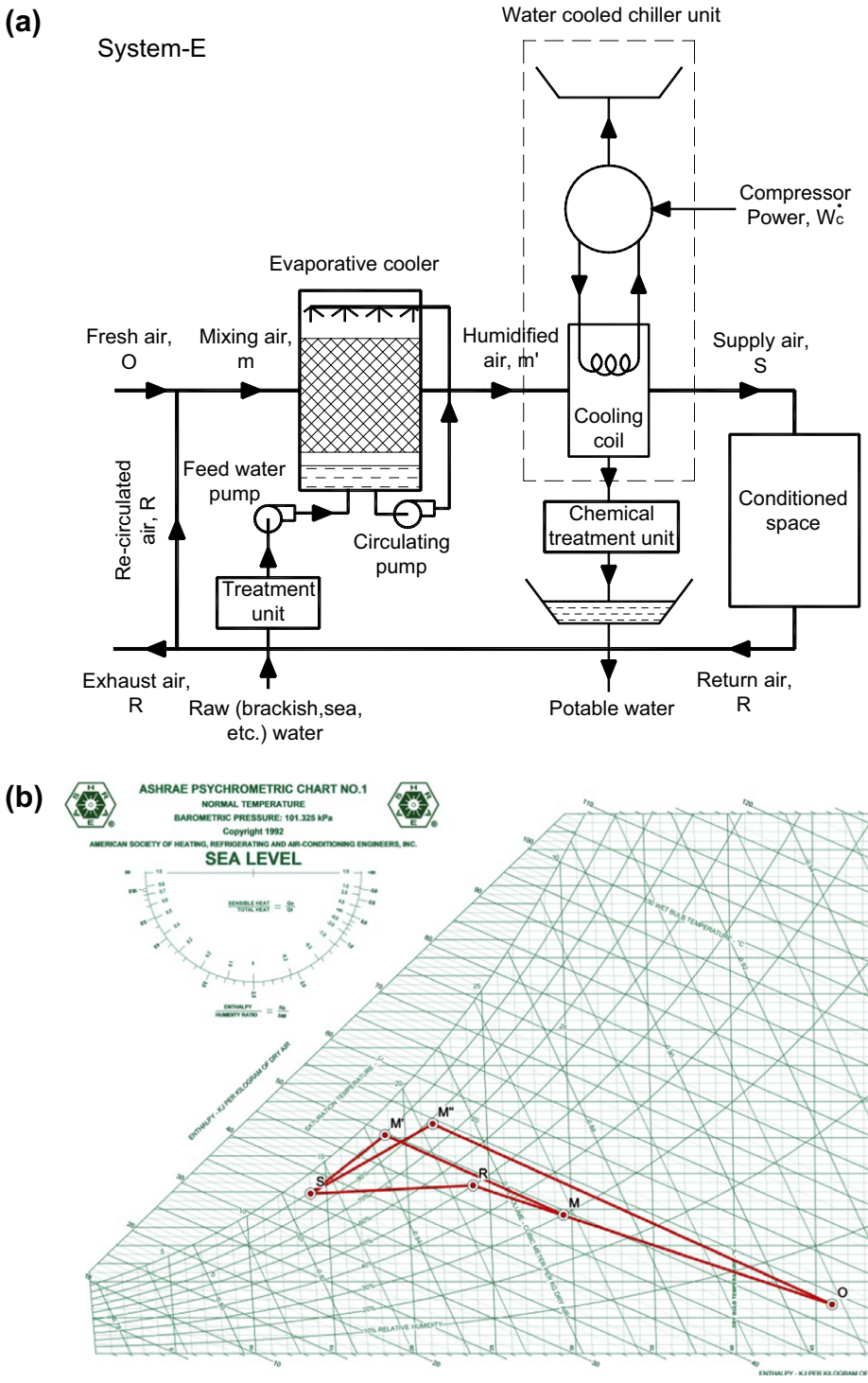

Fig. 5. Schematic and psychometric diagrams of proposed system-E: (a) schematic, (b) psychometric chart.

The air specific humidities and enthalpies that illustrated in Eqs. (1)–(4) are calculated from air properties. Air conditioning system power consumption (compressor work), conditioned air properties after humidifier and heat recovery, properties of state of air supplied to conditioned space, steam humidifier electrical power, and saving in power consumption of proposed systems are calculated from the following equations:

$$COP = \frac{\dot{Q}_{c.c}}{\dot{W}_c} \tag{5}$$

$$\eta_h = \frac{T_i - T_o}{T_i - T_{wb}} \tag{6}$$

$$\varepsilon_{HR} = \frac{\dot{m}_a(\Delta i)_{fresh\ air}}{\dot{m}_{\min}(\Delta i)_{max}} \tag{7}$$

$$RSHF = \frac{Cp_a(T_R - T_s)}{(i_R - i_s)} \tag{8}$$

$$\dot{E}_{steam,h} = \dot{m}_{steam} * h_{fg} \tag{9}$$

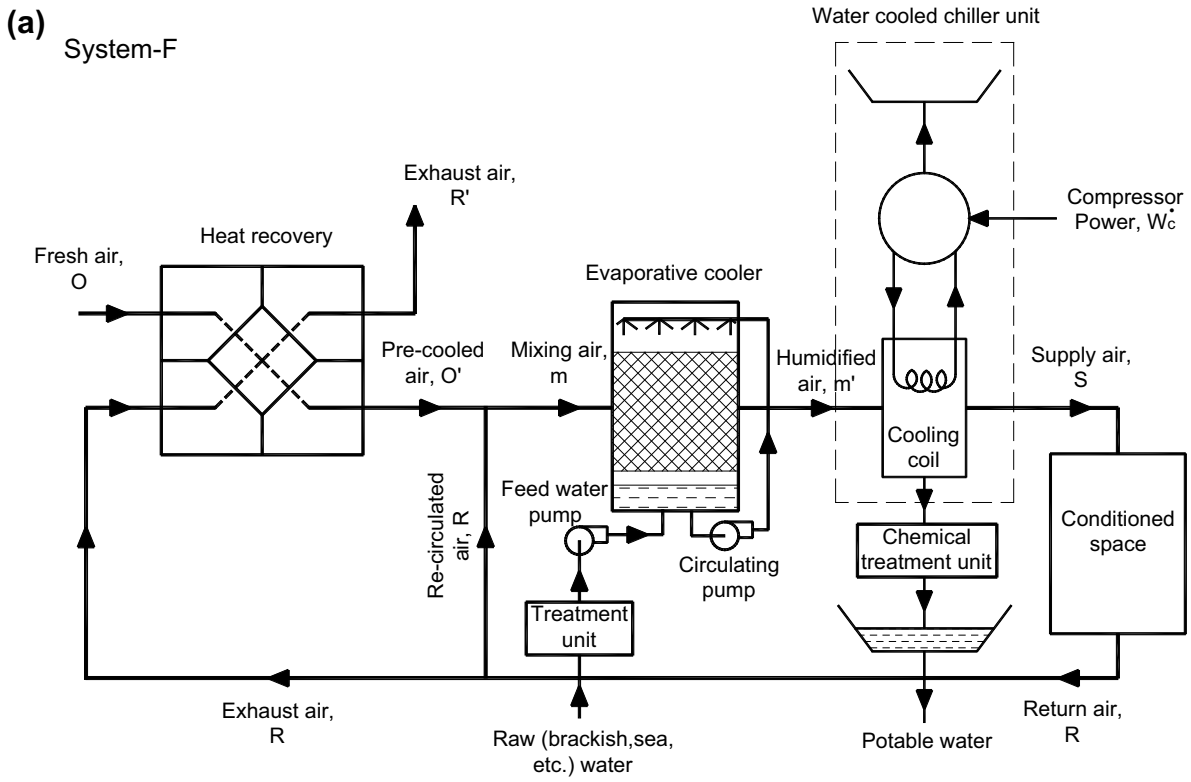

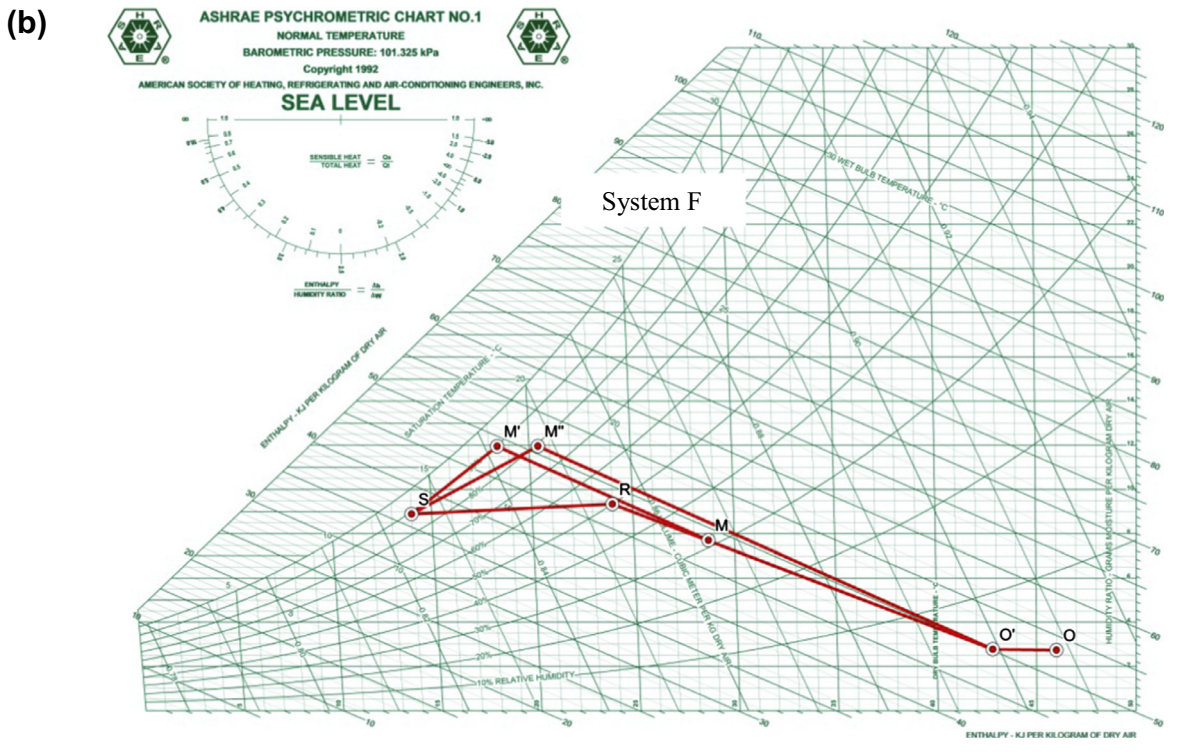

Fig. 6. Schematic and psychometric diagrams of proposed system-F: (a) schematic, (b) psychometric chart.

$$\dot{E}_{BS} = \dot{W}_c + \dot{E}_h \quad (10)$$

$$\dot{E}_{PS} = \dot{W}_c + \dot{E}_{pump} \quad (11)$$

$$Power\,Saving\,\% = \frac{\dot{E}_{BS} - \dot{E}_{PS}}{\dot{E}_{BS}} \quad (12)$$

$$\dot{m}_{feed,w} = \dot{m}_a(w_{a,o,evc} - w_{a,i,evc}) \quad (13)$$

$$R = \frac{\dot{m}_w}{\dot{m}_{feed,w,c.c}} \quad (14)$$

The studied parameters, $\dot{m}_w, \dot{Q}_{c.c}, \dot{E}_{BS}, \dot{E}_{PS}$, and percentage of power saving are calculated at the following different operating variables ranges which are typical operating conditions of the hot and dry climatic regions:

Fresh air mixing ratio 0.05–1

Conditioned space supply air temperature 12–16 °C

Ambient wet-bulb temperature 18–23 °C

Ambient design dry-bulb temperature 46 °C

4. Results and discussions

The present work is carried out to analyze the performance of different proposed modified large scale hybrid air conditioning and HDD systems for hot and dry climatic areas driven by water cooled chiller unit. In this study, the effects of different system operating parameters such as fresh air ratio, outside dray bulb temperature and supply air temperature on $\dot{m}_w, \dot{Q}_{c.c}, \dot{E}_{BS}, \dot{E}_{PS}$, power saving %, and total cost saving (TCS) are investigated.

Exploration runs are firstly performed to be sure from the relation between fresh water production rate $\dot{m}_w$ and the total electrical power consumption $\dot{E}_{PS}$ of the proposed systems and the conditioned space cooling load, $\dot{Q}_R$. The results of these runs as shown in Fig. 7 reveal a linear relation between $\dot{m}_w$ & $\dot{E}_{PS}$ and $\dot{Q}_R$. This means that (i) if the room cooling load increased or decreased by a certain percentage, the water production rate and the electric power consumption will increase or decrease by the same percentage, and (ii) the trends obtained for the variation of $\dot{m}_w$, $\dot{Q}_{c.c}$, $\dot{E}_{BS}$, $\dot{E}_{PS}$ with the controlling parameters (fresh air ratio, outside dry bulb temperature and supply air temperature) are valid for any value of $\dot{Q}_R$. Therefore, the present study is carried out at specified selected value of $\dot{Q}_R = 1000$ TR. Results for other values of $\dot{Q}_R$ can be obtained by multiplying the results obtained in the present result by $(\dot{Q}_R/1000)$.

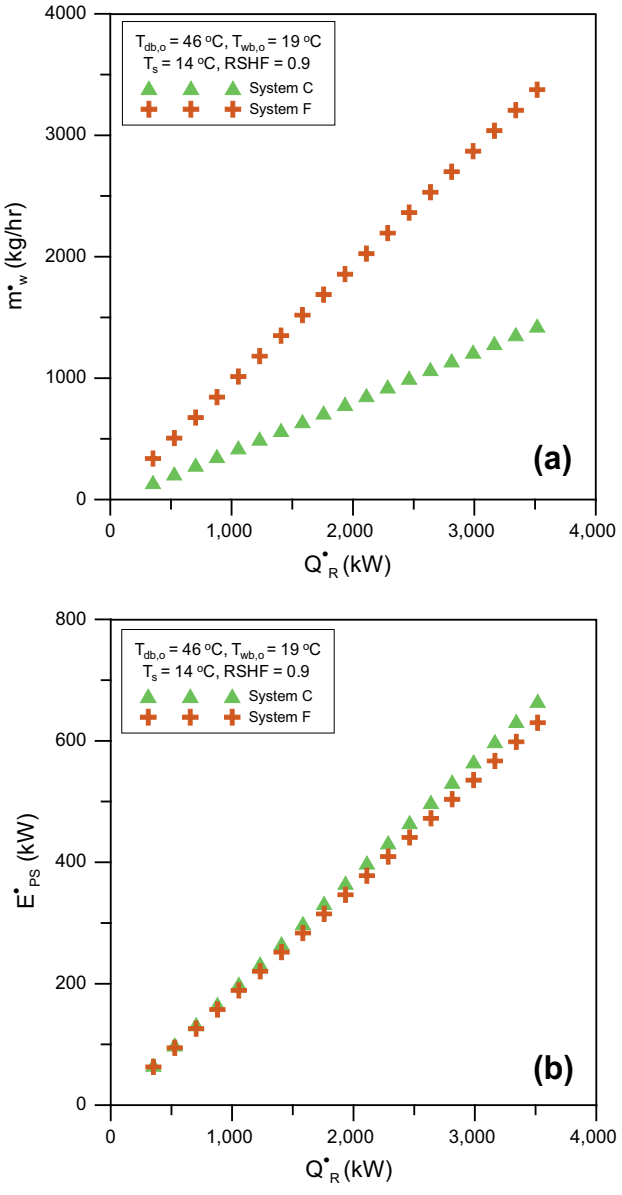

Fig. 7. Influence of conditioned space cooling load on: (a) $\dot{m}_w$, (b) $\dot{E}_{PS}$.

4.1. Effects of percentage of fresh air

Fig. 8a–e shows the variation of $\dot{m}_w$, $\dot{Q}_{c.c}$, $\dot{E}_{BS}$, $\dot{E}_{PS}$, power saving percentage against fresh air ratio $(\dot{m}_o/\dot{m}_s)$ for the different studied systems (system-A to system-F) at $T_{wb,o}$ = 19 °C and T_s = 14 °C. Fig. 8a shows that the fresh water production rate $\dot{m}_w$ increases for system-E, remarkably increases for systems C & D, and approximately remains constant for system-F with increasing the fresh air ratio. This can be investigated with the aid of Figs. 3b–6b and Eq. (1) as follows: (i) in system-E and with maintaining values of T_s & η_h, increasing the fresh air ratio makes point M to moves towards point O on the line OR (Fig. 5b) and this reduces specific humidity of point M and slightly increase the specific humidity of point M' and in turns increases water production rate as per Eq. (1). (ii) in systems- C and D, $\dot{m}_w$ increases due to moving of point M towards point M′ in system-C (Fig. 3b) and towards point O″ in System D (Fig. 4b) increasing its moisture content which leads to the increase of water production rate as per Eq. (1). The reduction of water production rate obtained from system-D than system-C is attributed to the dropping of the wet bulb at humidifier inlet (O′) due to using heat recovery unit and this reduces the specific humidity of point m in Fig. 4b to be lower than that of point m in Fig. 3b which in turn decreases water production rate as per Eq. (1). In system-F, the increase in the humidity of point M′ due to moving of point M away from point R with increasing fresh air ratio is balanced with the reduction in the humidity of point M′ due to the decrease of the wet bulb temperature of point O′ with increasing fresh air ratio and this makes $\dot{m}_w$ approximately constant. Furthermore, systems E and F produce higher fresh water production rate than systems C and D due to the location of humidifier in the system. Locating the humidifier after the mixing section (systems E and F) increases the air mass flow rate passing on the humidifier leading to high specific humidity of point m′ that leads to higher water production rate. Fig. 8a also shows that the reduction of the water production rate of systems C and D than systems E and F decreases with increasing fresh air ratio until completely vanishing at 100% fresh air ratio. This can be attributed to the reduction of the by passed air across the humidifier for systems C and D with increasing fresh air.

Fig. 8b shows the variation of $\dot{Q}_{c.c}$ with fresh air ratio for the basic systems in comparable with the modified proposed systems. As shown in the figure, the cooling coil capacity of the modified systems is considerably lower than that of the basic systems due

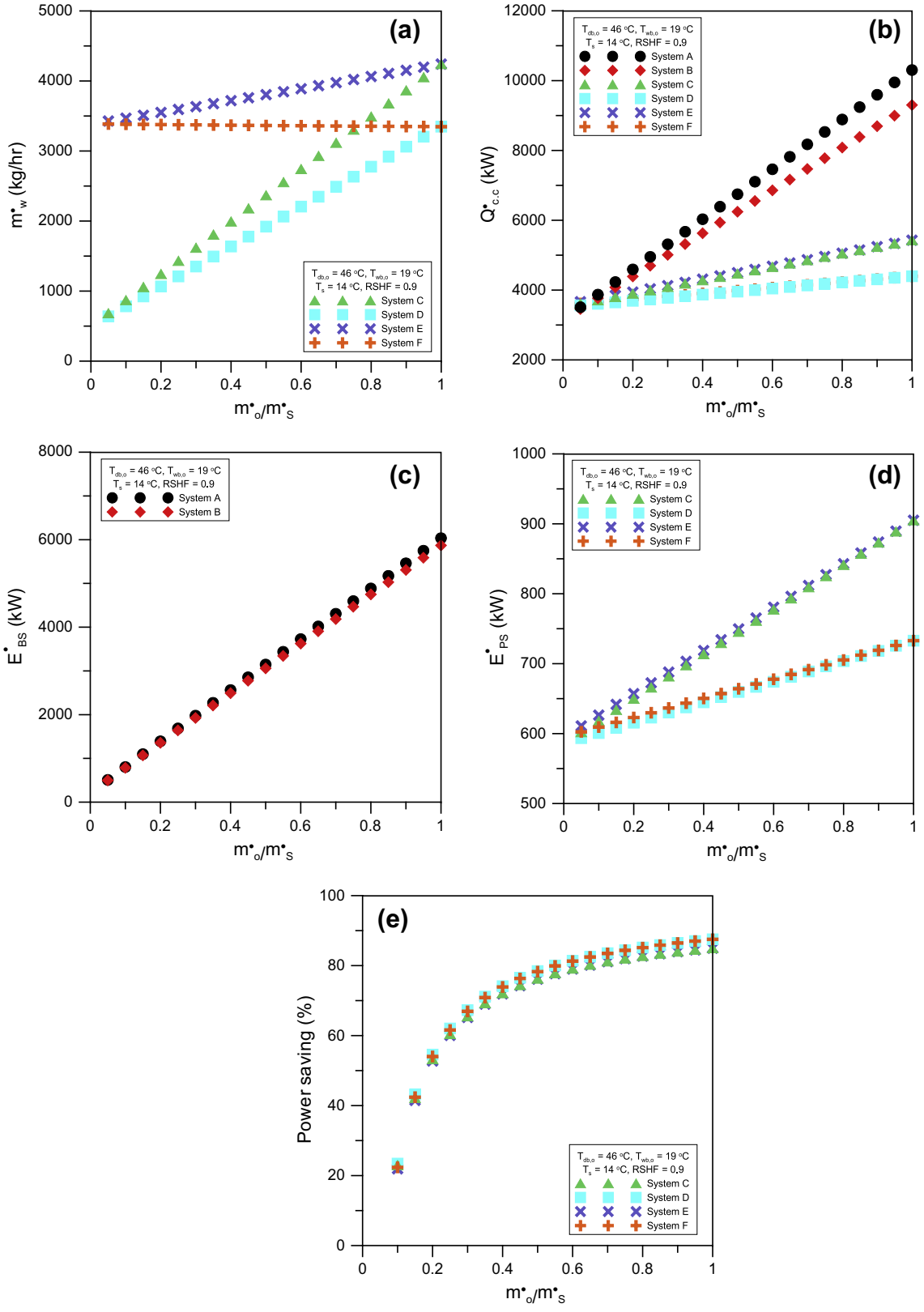

Fig. 8. Influence of mixing ratio on: (a) m_w, (b) $Q_{c.c}$ for all systems, (c) E_{BS} for basic systems, (d) E_{PS} for proposed systems, (e) Power saving %.

to the pree free cooling of the air in the evaporative cooler which reduces the enthalpy at inlet of the cooling coil. The figure also shows that systems with heat recovery unit (system-B, system-D and system-F) have lower cooling capacities compared with corresponding systems without heat recovery units (system-A, system-C and system-F), respectively. This can be attributed to

the free cooling obtained by cooling of fresh air by exhaust air. Figs. 8b also shows that the location of the evaporative cooler in the system (system C as compared to system F and system D as compared to system F) has no effect on the cooling capacity. Fig. 8b also shows that the cooling coil capacity increases considerably with $(\dot{m}_o/\dot{m}_S)$ in basic systems A and B, but moderately increases for proposed systems C, D, E, and F. This can be attributed to increasing the air enthalpy at the inlet of cooling coil with increasing the fresh air ratio. The existence of evaporative cooling in the proposed systems damps the increase of the cooling coil capacity with the fresh air ratio. The figure also shows that at low fresh air ratio (less than 15%) the reduction of the cooling coil capacity due to the existence of the evaporative cooler and heat recovery is very small and in this case it is not feasible to use them. However, increasing the fresh air ratio increases the percentage of reduction in the cooling capacity due to using evaporative cooler and heat recovery and the feasibility of using them improves.

Fig. 8c and d show the total electrical power usage E_{BS}, E_{PS} for basic and proposed systems with variation of $(\dot{m}_o/\dot{m}_S)$, respectively. As illustrated in the figures E_{BS} and E_{PS} have the same trends of $Q_{c.c}$ according to Eq. (5) where COP is constant for water cooled chiller. Fig. 8c shows that the utilization of heat recovery in system-B causes two opposite effects; reduction in compressor energy consumption and increasing in steam humidifier energy consumption. The reduction in the compressor power is slightly overcome on the increase in humidifier power and this leads to the converge of the total energy consumption E_{BS} for systems A and B at any $(\dot{m}_o/\dot{m}_S)$. This means that in hot and dry regions, the feasibility of using heat recovery for energy saving is not verified.

Power saving percentage versus $(\dot{m}_o/\dot{m}_S)$ is presented in Fig.8e. As shown in figure, the percentage of the power saving of the proposed systems increases remarkably with $(\dot{m}_o/\dot{m}_S)$ up to $(\dot{m}_o/\dot{m}_S) = 0.7$, after that the power saving slightly increases and the deviation is within 4.7%. Moreover, Fig. 8e shows that the difference in power saving between the proposed systems is small at any fresh air ratio. This is attributed to the small differences in E_{PS} for the different proposed systems compared with E_{BS} as can be seen in Fig 8c and d.

4.2. Effects of supply air temperature

Fig. 9a–e shows the variation of $\dot{m}_w$, $Q_{c.c}$, E_{BS}, E_{PS}, percentage of power saving against air supply temperature to the conditioned space (T_s) for all studied systems at $T_{wb,o} = 19$ °C and $(\dot{m}_o/\dot{m}_S) = 25\%$. Fig. 9a shows that the fresh water production rate, $\dot{m}_w$ increases with increasing T_s for all systems. This can be attributed to that the increase in T_s reduces the enthalpy difference across the conditioned space and hence increases the supply air flow rate necessary to carry up the cooling load. Increasing the supply air flow rate increases the fresh water production rate as per Eq. (1) in spite of the increase of the specific humidity of point S (Figs. 4 and 6) with increasing T_s. Fig. 9a also shows that the difference in water production rate due to using heat recovery (between systems C and D and systems E and F) diverges with increasing T_s.

Fig. 9b shows the variation of $Q_{c.c}$ with T_s for basic systems in comparable with modified proposed systems. As shown in the figure, $Q_{c.c}$ increases with increasing T_s for all the systems. The rate of increase of $Q_{c.c}$ with T_s for basic systems is higher than that of the proposed systems. The increase of $Q_{c.c}$ with Ts is attributed to the increase of supplied air flow rate and consequently the increase of the fresh air flow rate which leads to the increase of the fresh air load and consequently the cooling coil load (cooling coil load = Conditioned space load which is constant + Fresh air load). The existence of evaporative cooling damping the increase of the fresh air load with increasing T_s and this attribute the smaller increase rate of cooling coil load with T_s for the proposed system as compared with the basic systems.

Fig. 9c and d show the variation of the total electrical power usage E_{BS}, E_{PS} for basic and proposed systems with T_s, respectively. As shown in the figures E_{BS} and E_{PS} have the same trends of $Q_{c.c}$ as per Eq. (5) where COP is constant. Against expectation, Fig. 9c shows that E_{BS} for systems B is a little bit lower than that of system B at any T_s and in spite of using heat recovery in system B. This can be attributed to the same explanation of Fig. 8c. Power saving percentage versus T_s is presented in Fig. 9e, as shown in figure the power saving of the proposed systems increases significantly with T_s. For example, the power saving improved by 12% with increasing T_s by 4 °C for all systems. Moreover, the differences in power saving between the proposed systems is small at any T_s, this is due to the small difference in E_{PS} compared with E_{BS} as can be seen in Fig. 8c and d.

4.3. Effects of ambient wet-bulb temperature

Fig. 10a–e shows the variation of $\dot{m}_w$, $Q_{c.c}$, E_{BS}, E_{PS}, and power saving percentage versus ambient wet bulb temperature $(T_{wb,o})$ for the studied systems at $T_s = 14$ °C and $(\dot{m}_o/\dot{m}_S) = 25\%$. Fig. 10a shows that the fresh water production rate, $\dot{m}_w$ increases with increasing $T_{wb,o}$ for all systems. This is attributed to the increase of the specific humidity of the air at the system inlet and in consequence at the inlet of the cooling coil with the increase of $T_{wb,o}$.

Fig. 10b shows the variation of $Q_{c.c}$ with $T_{wb,o}$ for basic systems in comparable with modified proposed systems. As shown in the figure, $Q_{c.c}$ decreases with $T_{wb,o}$ for basic system B but it is nearly constant for basic system A. On the other hand $Q_{c.c}$ increases with $T_{wb,o}$ for all proposed systems. The reduction of $Q_{c.c}$ with $T_{wb,o}$ for basic system B can be attributed to the presence of heat recovery which cause a reduction of the enthalpy of mixing point M′ with the increase of $T_{wb,o}$ (Fig. 2b) and consequently decreasing the enthalpy difference across the cooling coil. On the other hand, for System A, the enthalpy of mixing point M' changes slightly with $T_{wb,o}$ (Fig. 1b) and therefore the cooling coil capacity is remains constant with increasing $T_{wb,o}$. Conversely, increasing of $Q_{c.c}$ with $T_{wb,o}$ for all proposed systems is due to the increase of fresh air latent heat which leads to the increase of cooling coil latent heat part and consequently the increase of the total capacities.

Fig. 10c and d show the variation of the total electrical power usage E_{BS}, E_{PS} with variation of $T_{wb,o}$ for basic and proposed systems, respectively. As shown in the figures E_{BS} andE_{PS} have the same trends of $Q_{c.c}$ as COP is constant. Unlike $Q_{c.c}$, Fig. 9c shows the remarkable decrease of E_{BS} with increasing of $T_{wb,o}$ for System A. This is attributed to the reduction/elimination of the power of the steam humidifier with increasing $T_{wb,o}$.

The variation of the percentage of Power saving with $T_{wb,o}$ is depicted in Fig. 10e. As shown in the figure the percentage of the power saving of the proposed systems decreases significantly with increasing $T_{wb,o}$, and it drops to 0% with increasing $T_{wb,o}$ to 22.5 °C for all systems where E_{BS} becomes equals to E_{PS}. This means that using evaporative cooler with energy recovery for power saving becomes unfeasible at $T_{wb,o} > 22.5$ °C. However using evaporative cooler with energy recovery unit becomes more feasible with decreasing $T_{wb,o}$; for example, the percentage of power saving becomes 67% at $T_{wb,o} = 18$ °C.

4.4. Feed and recovery water rates

The water recovery rate (R) is calculated rom Eq. (13) as the ratio between the fresh water production rate Eq. (1) and the

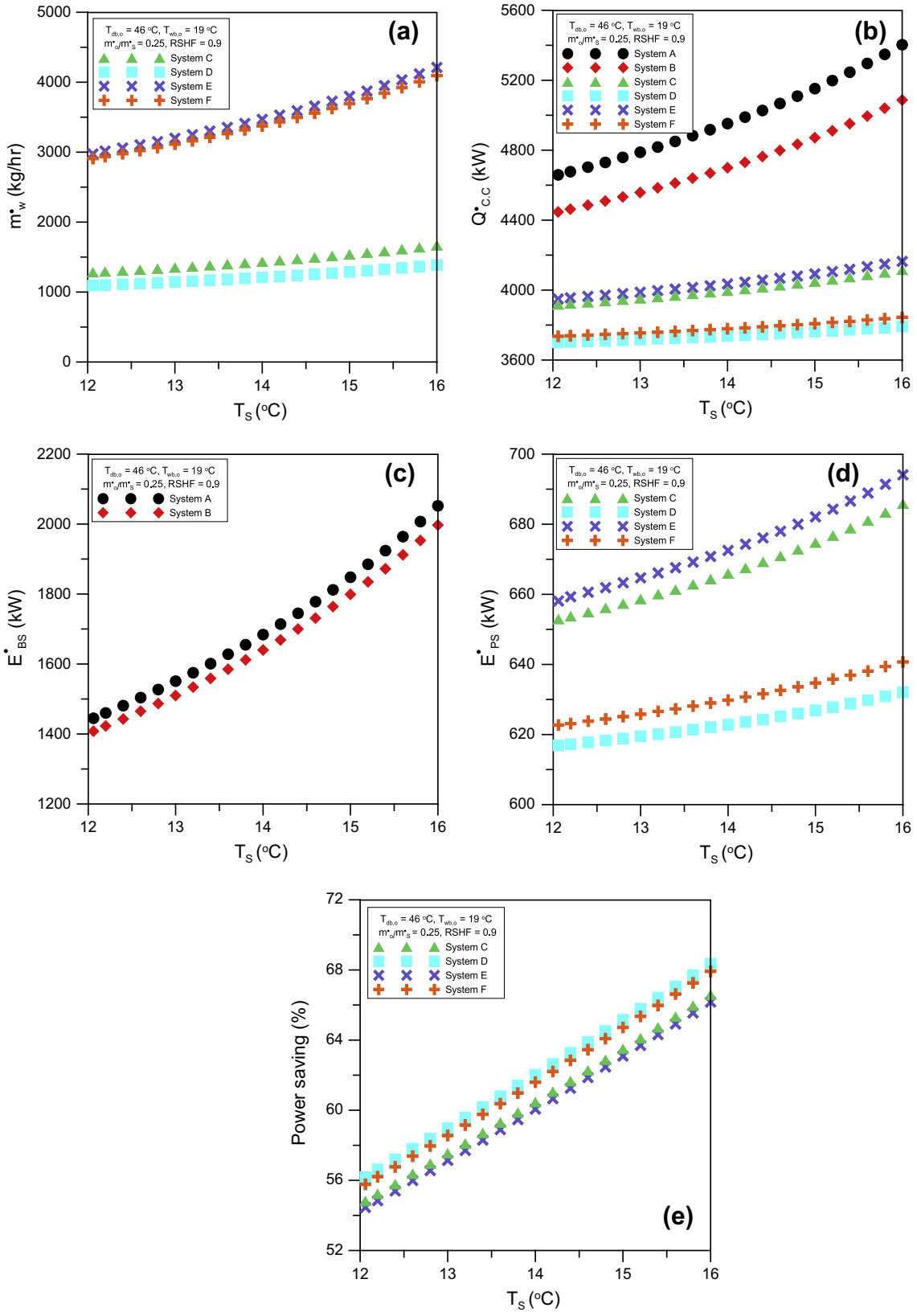

Fig. 9. Influence of space supply air temperature on: (a) $\dot{m}_w$, (b) $\dot{Q}_{c.c}$ for all systems, (c) $\dot{E}_{BS}$ for basic systems, (d) $\dot{E}_{PS}$ for proposed systems, (e) %Power saving.

feed water rate Eq. (12). The feed water rate in Eq. (12) is the water vapor carried up with the air in the evaporative cooler. In hot and dry regions, part of the feed water is utilized in the adjusting the relative humidity of the conditioned space and the other part condenses on the cooling coil and produces the fresh water. Make up water is required to be added to the evaporative cooler to substitute this feed water as well as the drain water.

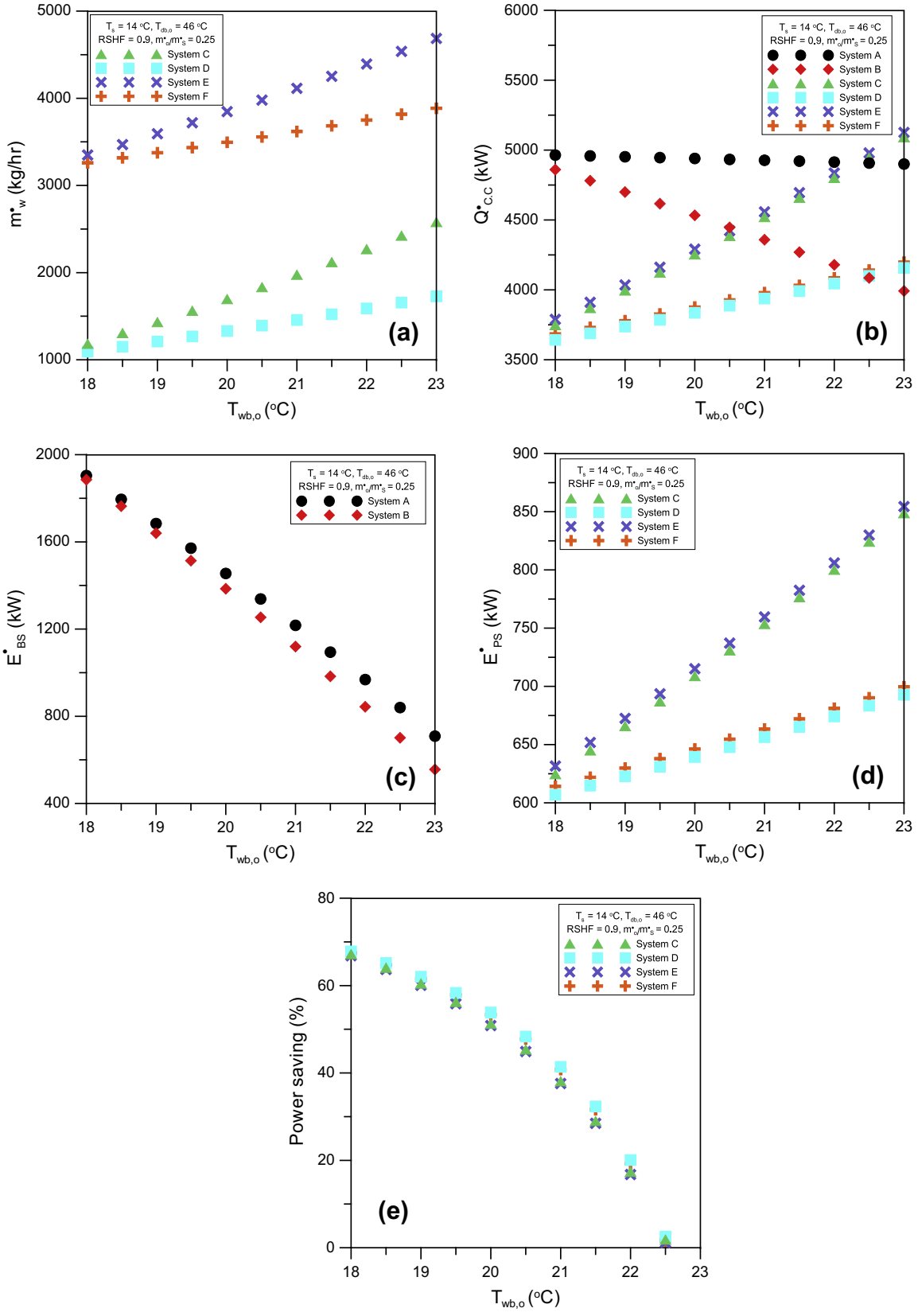

Fig. 10. Influence of outside air wet bulb temperature: (a) $\dot{m}_w$, (b) $\dot{Q}_{c.c}$ for all systems, (c) E_{BS} for basic systems, (d) E_{PS} for proposed systems, (e) %Power saving.

Fig. 11 shows the variation of the feed water flow rate and the water recovery rate with fresh air ratio (m_o/m_S), supply air temperature T_s and ambient wet bulb temperature $T_{wb,o}$ for the different proposed systems. The figure shows that for all the proposed systems, the feed water rate increases with increasing $(m_o/m_S)$and T_s and decreasing $T_{wb,o}$. This is attributed to the increase of the

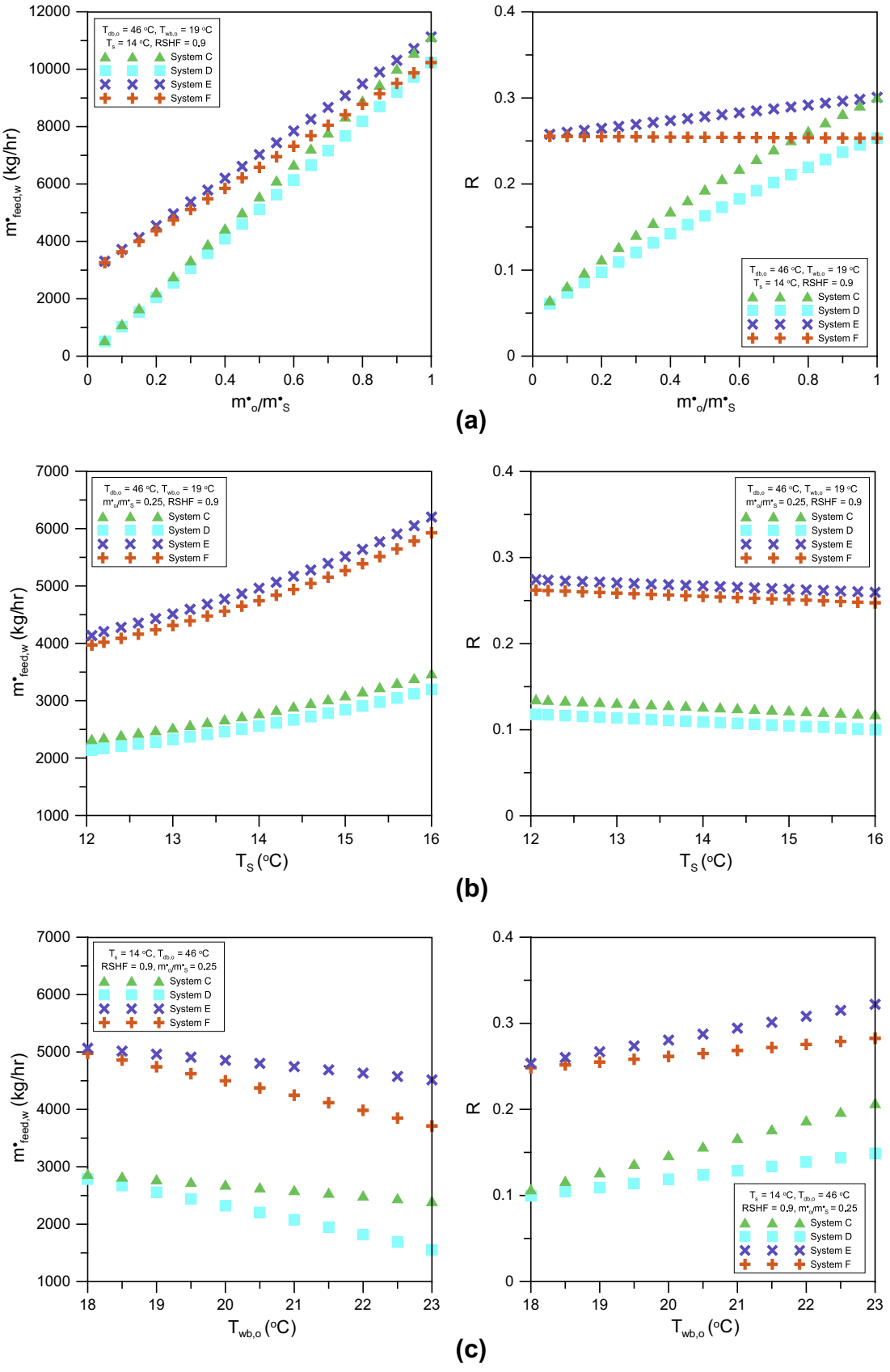

Fig. 11. Variation of feed water rate and water system recovery for proposed systems with: (a) fresh air ratio, (b) T_s, (c) $T_{wb,o}$.

capability and capacity of the air passing in the evaporative cooler to carry up water vapor with the increase of $(\dot{m}_o/\dot{m}_S)$and T_s and decrease of $T_{wb,o}$. The figure also shows that the feed water flow rates of systems E and F are higher than those of systems C and D, respectively. This is attributed to that in systems E and F all the supply air flow rate is passing on the evaporative cooler but in systems C and D only the fresh air is passing on the evaporative cooler and carrying up smaller water vapor than the supply air.

Fig. 11 shows that for all the proposed systems, the water recovery rate (R) increases with increasing $(\dot{m}_o/\dot{m}_S)$ and $T_{wb,o}$ and decreasing T_s. This is attributed to (i) the increase of the capability and capacity of the air passing in the evaporative cooler to carry up water vapor with the increase of $(\dot{m}_o/\dot{m}_S)$, (ii) increasing $T_{wb,o}$ means the decrease of the water vapor needed to adjust the relative humidity inside the conditioned space and consequently increases the water production rate, and (iii) decreasing T_s means increasing the capacity of the cooling coil to condenses water on it producing more fresh water. The figure also shows that the recovery rate (R) systems E and F are higher than those of systems C and D, respectively. This is attributed to the increase of the specific humidity of the air entering the cooling coil in systems E and F compared to those of systems C and D. Increasing the specific humidity on the cooling coil increases the water condensate rate and consequently produces more fresh water.

Fig. 11 also shows that using heat recovery units (system D and F) slightly decrease the feed water rate and the recovery rate as compared to the systems without heat recovery (system C and E). This can be attributed to the decrease of the temperature of air entering on the evaporative cooler with using heat recovery. Decreasing air entering temperature on the evaporative cooler decreases its capacity to carry up water vapor and consequently decreases the specific humidity of the air entering the cooling coil and both cause the decrease of the feed water rate and the water recovery rate, respectively.

4.5. System selection and cost analysis

The analysis and discussion of Sections 4.1–4.3 reveals that (i) the maximum energy saving and max water production rate depends on the operating conditions $(\dot{m}_o/\dot{m}_S)$, T_s and $T_{wb,o}$, (ii) the operating conditions at which the maximum energy saving occurs is different than the one at which the maximum water production occurs, and (iii) at a certain operating conditions, the system that have maximum energy saving may be different than the one that gives maximum water production rate. Therefore, the optimum system at certain operating conditions should be selected based on the sum of the cost savings obtained due to energy saving and fresh water production. For this reason, the total cost saving (TCS) value ($/h) which considers both costs savings due to system power saving and fresh water production is proposed and used for systems comparisons and optimal system selection. TCS can be calculated from the following equation:

$$TCS\ (\$/h) = \dot{m}_w \times \textit{Water unit rate}\ (\$/m^3) + (\dot{E}_{BS} - \dot{E}_{PS}) \times \textit{Electricity unit rate}\ (\$/kW\,h) \quad (13)$$

The electricity and water unit rates differ from a city to another. In this study typical values of electricity and water unit rates 0.02 $/(kW h) and 2.5 $/m^3 of Gulf cities [15] are considered.

Fig. 12a–c shows the variation of TCS against $(\dot{m}_o/\dot{m}_S)$, T_s, and $T_{wb,o}$ for all proposed systems. Fig. 12-a shows that TCS increases with increasing fresh air ratio for all systems and this can be attributed to the increase of both of the fresh water production and the energy saving with the increase of fresh air ratio as shown

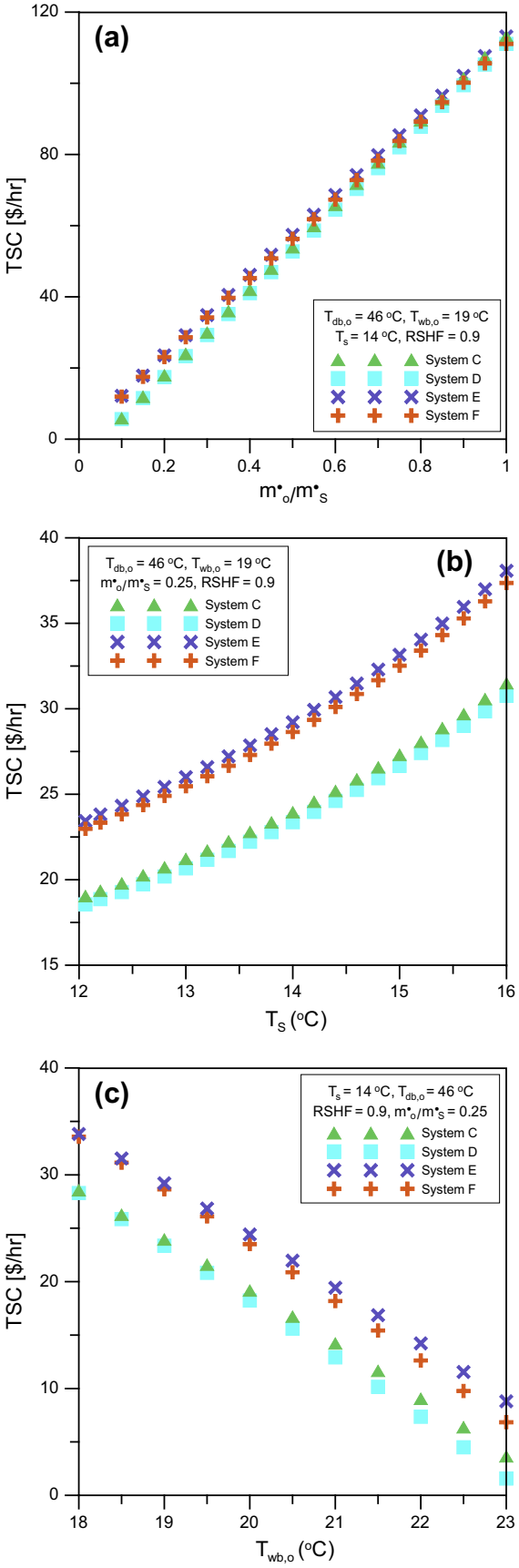

Fig. 12. Variation of TCS for proposed systems with: (a) fresh air ratio, (b) T_s, (c) $T_{wb,o}$.

in Fig. 8a. Fig. 12a also shows that at low fresh air ratio, the total cost saving in systems E and F is higher than those of systems C and D. The differences in cost savings between systems E & F and C & D, respectively vanishes with increasing the fresh air ratio until all the systems become having the same TCS at 100% fresh air.

Fig. 12b shows that for all proposed systems, TCS increases with the increase of the supply air temperature T_s. The trend is the same for all fresh air ratios and outside air wet bulb temperatures. Increasing TCS with the increase of the supply air temperature can be attributed to the increase of the supply air and fresh air flow rates with increasing T_s. Increasing the supply and fresh air flow rates increase both of the fresh water production rate and the energy saving which lead to the increase in TCS. Fig. 12b also shows that at any T_s, system E has the highest TCS, then system F, then system C and finally system D. This can be attributed to the remarkable higher water production rates of systems E and F, as shown in Fig. 9a, and the slightly higher power saving of systems D and F, as shown in 9-e. It worth to mention that the trends and comparisons of the TCS of the different systems that are shown in Fig. 12b may be changed with the changes of the considered water price and energy price rates.

Fig. 12c shows that for all proposed systems, TCS decreases with the increase of the outdoor wet bulb temperature $T_{wb,o}$ at 25% fresh air ratio and T_s = 14 °C. The trend is the same for all fresh air ratios and supply air temperatures. Decreasing the TCS with the increase of the outdoor air wet bulb temperature can be attributed to the remarkable decrease of the power saving with the increase of the outdoor wet bulb temperature as shown in Fig. 10e. Decreasing TCS with the increase of $T_{wb,o}$ due to the decrease of the power saving overcomes on the increase of the TCS due to the increase of the water production rate (see Fig. 10a). This means that, the decrease of the power saving is the dominant. It is also worth to mention that the trends of the TCS with the outdoor wet blub temperature that is shown in Fig. 12c may be changed with the changes of the water and energy units rates. Fig. 12c also shows that at any $T_{wb,o}$, system E has the highest TCS, then system F, then system C and finally system D. This can be attributed to the discrepancies in water production rates of the different systems with the same value of the power saving as shown in Figs. 10a and b, whereas system E has the highest water production rate then system F, then system C and finally system D.

To have a feeling of the quantities of water production rate, energy consumption rate, energy saving and total cost saving rates of this optimal system (system E), these rates are tabulated in Table 1 for different projects of different rooms cooling capacities at 25% fresh air ratio, 14 °C supply air temperature and 19 °C wet bulb temperature. As shown in the table, a considerable water production rates and energy saving can be obtained especially for large projects of high cooling load. As shown in the table, the water production rate and energy saving leads to huge saving in the running cost for buildings operation. For example for a project of 10,000 TR cooling load, the system can produce a daily cost saving of 7012 $ per day. Decision regarding using the proposed systems should be conducted based on the payback period of the extra initial cost of system E over basic system B. Rough estimation based on the extra equipment cost shows that the payback period is expected to be less than two years which leads to a recommendations of using these proposed systems for cost savings.

Table 1
Savings of system-E for different cooling loads (T_s = 14 °C, T_{wb} = 19 °C, $\dot{m}_a/\dot{m}_S$ = 0.25).

$\dot{Q}_R$ (TR)	$\dot{m}_w$ (Tone/day)	$\dot{E}_{PS}$ (kW)	Power saving (kW)	TCS ($/day)
100	9	67	101	70
500	43	336	506	351
1000	86	673	1016	701
2500	215	1681	2529	1753
5000	431	3363	5058	3506
10,000	862	6725	10,117	7,012
30,000	2587	20,175	30,350	21,035
50,000	4311	33,625	50,584	35,058
70,000	6036	47,075	70,818	49,081

4.6. Numerical correlations

To simplify and generalize the use of the results of the present study, the numerical results obtained for the proposed systems are regressed to predict correlations for $\dot{m}_w$ and $\dot{E}_{ps}$ in terms of $\dot{Q}_R$, $(\dot{m}_o/\dot{m}_S)$, $(T_s/T_{db,o})$, and $(T_{wb,o}/T_{db,o})$. The obtained correlations with errors ranges are presented in Table 2 for the four proposed systems. The predicted correlations are valid for the following ranges $0.05 \leqslant (\dot{m}_o/\dot{m}_S) \leqslant 1.0$, $12\ ^\circ\text{C} \leqslant T_s \leqslant 16\ ^\circ\text{C}$, and $18\ ^\circ\text{C} \leqslant T_{wb,o} \leqslant 23\ ^\circ\text{C}$. The correlations predictions are compared with the results of the present studies in Figs. 13 and 14. The figures also the deviation of the results from the correlations predictions.

Table 2
Numerical correlations prediction and errors of proposed systems.

Systems	Numerical correlations	Error range
System-C	$\dot{m}_w = 156.38 \times \dot{Q}_R \left(\frac{\dot{m}_a}{\dot{m}_s}\right)^{0.85} \left(\frac{T_s}{T_{db,o}}\right)^{1.28} \left(\frac{T_{wb,o}}{T_{db,o}}\right)^{3.76}$	This correlation predicts 86% of the numerical results within error ±10%
	$\dot{E}_{PS} = 4.20 \times \dot{Q}_R \left(\frac{\dot{m}_a}{\dot{m}_s}\right)^{0.29} \left(\frac{T_s}{T_{db,o}}\right)^{0.56} \left(\frac{T_{wb,o}}{T_{db,o}}\right)^{2.36}$	This correlation predicts 91% of the numerical results within error ±15%
System-D	$\dot{m}_w = 55.15 \times \dot{Q}_R \left(\frac{\dot{m}_a}{\dot{m}_s}\right)^{0.77} \left(\frac{T_s}{T_{db,o}}\right)^{1.20} \left(\frac{T_{wb,o}}{T_{db,o}}\right)^{2.41}$	This correlation predicts 86% of the numerical results within error ±10%
	$\dot{E}_{PS} = 0.78 \times \dot{Q}_R \left(\frac{\dot{m}_a}{\dot{m}_s}\right)^{0.138} \left(\frac{T_s}{T_{db,o}}\right)^{0.28} \left(\frac{T_{wb,o}}{T_{db,o}}\right)^{1.10}$	This correlation predicts 94% of the numerical results within error ±10%
System-E	$\dot{m}_w = 67.7 \times \dot{Q}_R \left(\frac{\dot{m}_a}{\dot{m}_s}\right)^{0.24} \left(\frac{T_s}{T_{db,o}}\right)^{1.29} \left(\frac{T_{wb,o}}{T_{db,o}}\right)^{2.71}$	This correlation predicts 85% of the numerical results within error ±15%
	$\dot{E}_{PS} = 4.16 \times \dot{Q}_R \left(\frac{\dot{m}_a}{\dot{m}_s}\right)^{0.29} \left(\frac{T_s}{T_{db,o}}\right)^{0.56} \left(\frac{T_{wb,o}}{T_{db,o}}\right)^{2.34}$	This correlation predicts 90% of the numerical results within error ±15%
System-F	$\dot{m}_w = 28.21 \times \dot{Q}_R \left(\frac{\dot{m}_a}{\dot{m}_s}\right)^{0.08} \left(\frac{T_s}{T_{db,o}}\right)^{1.25} \left(\frac{T_{wb,o}}{T_{db,o}}\right)^{1.49}$	This correlation predicts 87% of the numerical results within error ±10%
	$\dot{E}_{PS} = 0.78 \times \dot{Q}_R \left(\frac{\dot{m}_a}{\dot{m}_s}\right)^{0.13} \left(\frac{T_s}{T_{db,o}}\right)^{0.29} \left(\frac{T_{wb,o}}{T_{db,o}}\right)^{1.09}$	This correlation predict 94% of the numerical results within error ±10%

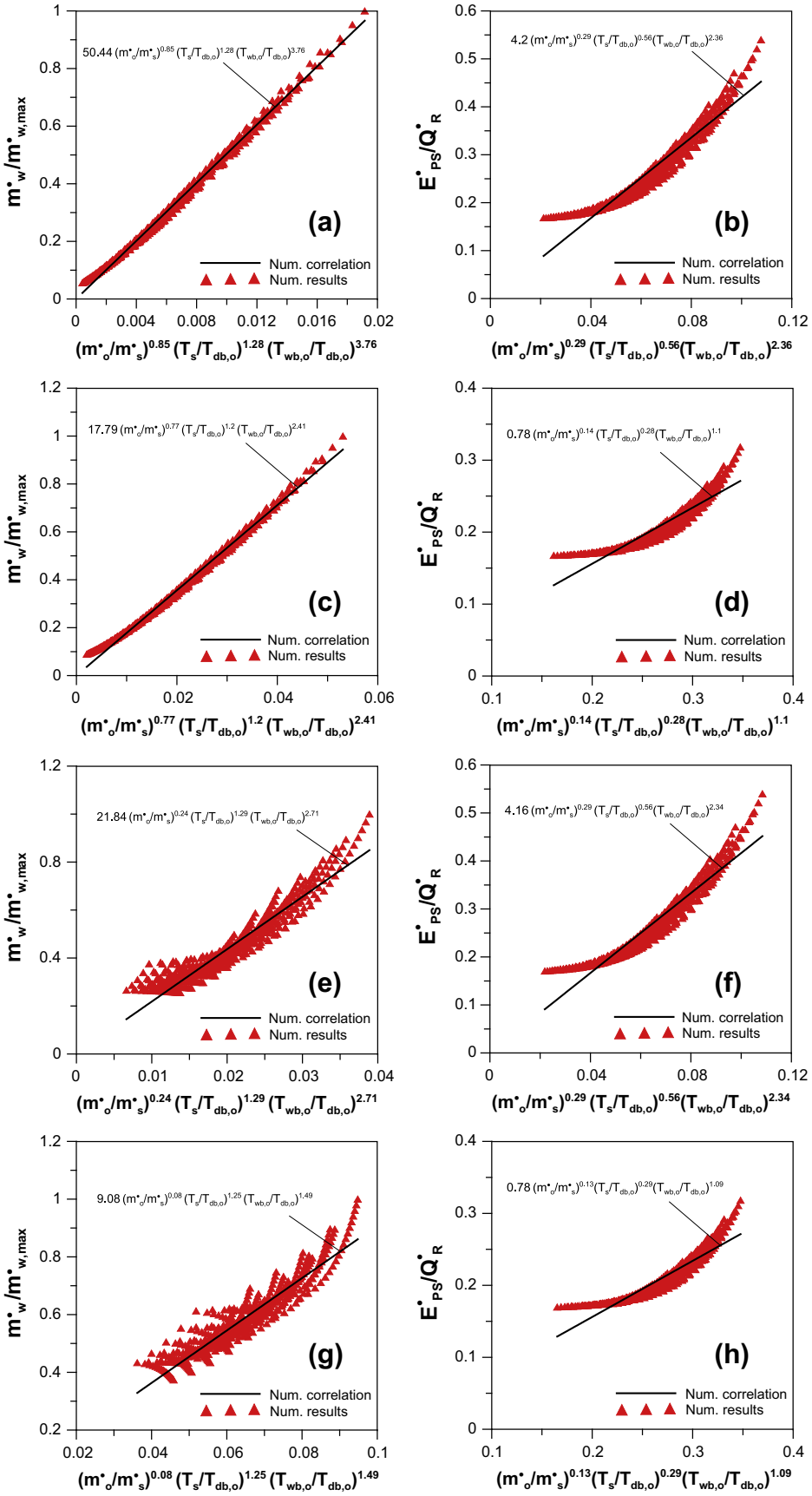

Fig. 13. Prediction of numerical correlations: (a & b) System-C, (c & d) System-D, (e &f) System-E, (g & h) System-F.

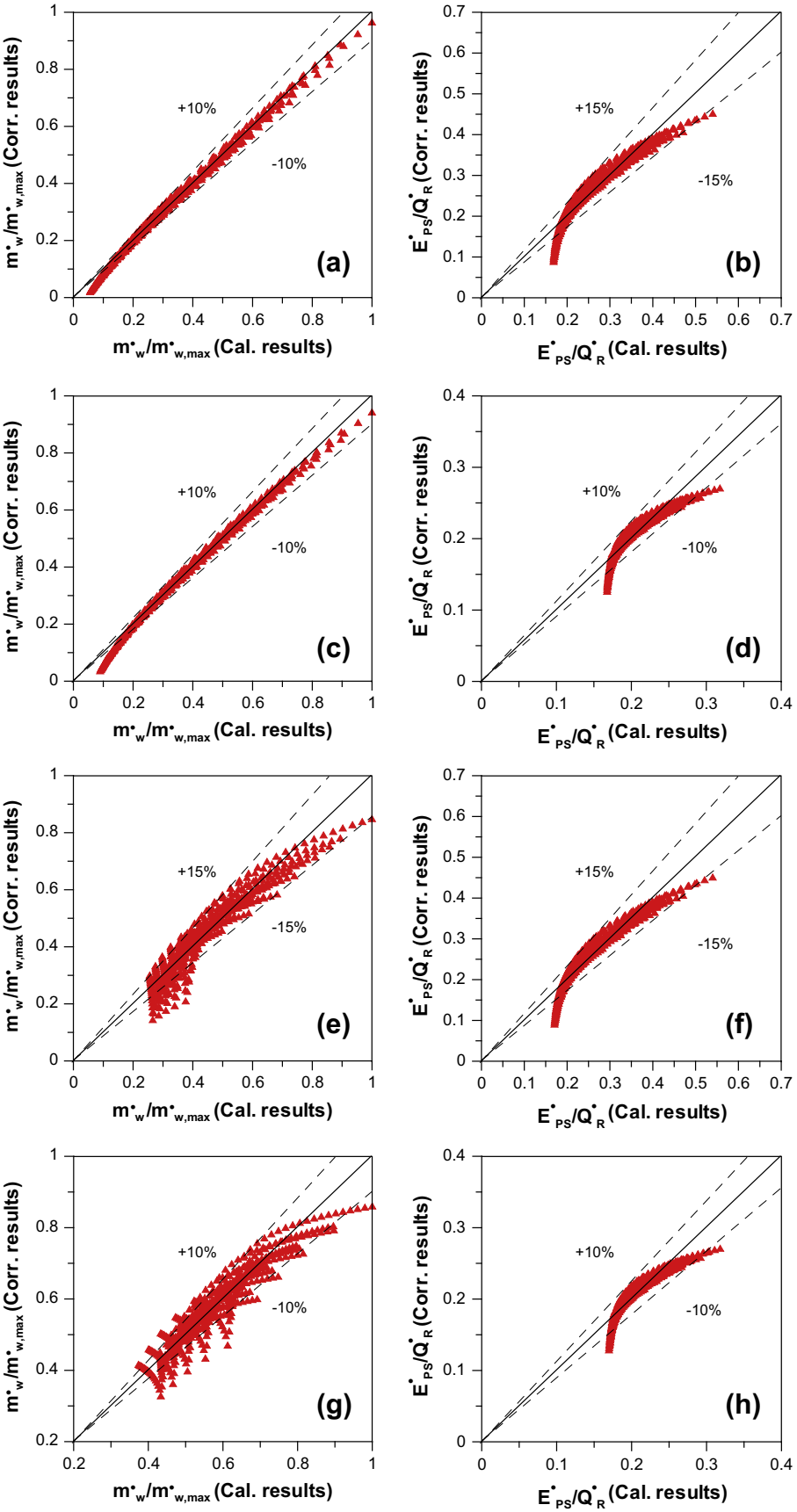

Fig. 14. Error of numerical correlations: (a & b) System-C, (c & d) System-D, (e & f) System-E, (g & h) System-F.

5. Conclusions

Theoretical investigating of the performance of proposed integrative air-conditioning (A/C) and humidification-dehumidification desalination (HDD) systems have been carried out for the purpose of energy saving of the air conditioning system and at the same time utilizing the system in fresh water production. Four systems are proposed with using heat recovery and evaporative cooling at different locations of the air conditioning systems. The influence of different system operating parameters (fresh air ratio, space supply air temperature, outside air wet bulb temperature) on the produced fresh water rate, refrigeration capacity, compressor power and percentage of power saving systems are investigated and presented for the four proposed systems. Evaluation and comparisons of the four systems based on the total cost saving in energy and fresh water production are presented. The conclusions obtained from the present study which can be considered as design guidelines are listed briefly in the following points:

- The fresh water production rate $m_w^{\cdot}$ increases with increasing fresh air ratio for systems C, D and E and it is approximately constant for system F.
- For all proposed systems, the fresh water production rate, $m_w^{\cdot}$ increases with increasing supply air temperature (T_s) and increasing outdoor wet bulb temperature.
- At any operating conditions (fresh air ratio, supply air temperature and outdoor air wet bulb temperature) the fresh water production rate of system E is higher than that of system F, the fresh water production rate of system F is higher than that of system C and the fresh water production rate of system C is higher than that of system D.
- Locating the evaporative cooling after the mixing of the fresh air with the return air (systems E and F) remarkably increase the water production rate as compared with the case of locating it on the fresh air side before the mixing point (systems C and D).
- Power saving of the proposed systems increases remarkably with increasing fresh air ratio until a value of 0.7 then it slightly increases with further increase of the fresh air ratio.
- Power saving of all the proposed systems increases with increasing the supply air temperature and decreasing the outdoor air wet bulb temperature.
- Numerical correlations for fresh water production rate, total system energy consumption and economical cost parameter are developed and presented in terms of studied parameters.
- At any operating conditions in the studied range ($0.05 \leqslant (m_o/m_s^{\cdot}) \leqslant 1.0, 12\ ^\circ\text{C} \leqslant T_s \leqslant 16\ ^\circ\text{C}$, and $18\ ^\circ\text{C} \leqslant T_{wb,o} \leqslant 23\ ^\circ\text{C}$) system D has the highest power saving, then system F, then system C, and finally system F.
- For all proposed systems, the total cost saving due to using evaporative cooler and heat recovery increases with the increase of the supply air temperature, and fresh air ratio and the decrease of the outdoor dry blub temperature.
- For units water and energy prices of 2.5 \$/m^3 and 0.02 \$/ (kW h) (Values of Golf cities) system E has the highest TCS, then system F, then system C and finally system D.

References

[1] A1-Juwayhel F, E1-Dessouky H, Ettouney H. Analysis of single-effect evaporator desalination systems combined with vapor compression heat pumps. Desalination 1997;114:253–75.
[2] Siqueiros J, Holland FA. Water desalination using heat pumps. Energy 2000;25:717–29.
[3] Slesarenko VV. Heat pumps as a source of heat energy for desalination of seawater. Desalination 2001;139:405–10.
[4] Al-Ansari A, Ettouney H, El-Dessouky H. Water–zeolite adsorption heat pump combined with single effect evaporation desalination process. Renewable Energy 2001;24:91–111.
[5] Narmine HA, El-Fiqi AK. Mechanical vapor compression desalination systems-a case study. Desalination 2003;58:43–150.
[6] Hawlader MNA, Dey PK, Diab S. Solar assisted heat pump desalination system. Desalination 2004;168:49–54.
[7] Chen J, Huang S. A discussion of heat pumps as a source of heat energy for desalination of seawater. Desalination 2004;169:161–5.
[8] Yuan G, Zhang L, Zhang H. Experimental research of an integrative unit for air conditioning and desalination. Desalination 2005;182:511–6.
[9] Gao P, Zhang L, Zhang H. Performance analysis of a new type desalination unit of heat pump with humidification and dehumidification. Desalination 2008;220:531–7.
[10] Wua JM, Huang X, Zhang H. Theoretical analysis on heat and mass transfer in a direct evaporative cooler. Appl Therm Eng 2008;29:980–4.
[11] Houab S, Lia H, Zhanga H. An open air–vapor compression refrigeration system for air-conditioning and desalination on ship. Desalination 2008;222:646–55.
[12] Wua JM, Huang X, Zhang H. Numerical investigation on the heat and mass transfer in a direct evaporative cooler. Appl Therm Eng 2009;29:195–201.
[13] Habeebullah BA. Performance analysis of a combined heat pump-dehumidifying system. JKAU Eng Sci 2010;21(1):97–114.
[14] Nada SA, Elattar HF, Fouda A. Experimental study for hybrid humidification–dehumidification water desalination and air conditioning system. Desalination 2015, in press (http://dx.doi.org/10.1016/j.desal.2015.01.032).
[15] Attia AAA. New proposed system for freeze water desalination using auto reversed R-22 vapor compression heat pump. Desalination 2010;254:179–84.
[16] Rane MV, Padiya YS. Heat pump operated freeze concentration system with tubular heat exchanger for seawater desalination. Energy Sustain Dev 2011;15:184–91.
[17] Jain JK, Hindoliy DA. Experimental performance of new evaporative cooling pad materials. Sustain Cities Soc 2011;1:252–6.
[18] Malli A, Seyf HR, Layeghi M, Sharifian S, Behravesh H. Investigating the performance of cellulosic evaporative cooling pads. Energy Convers Manage 2011;52:2598–603.
[19] Mehrgoo M, Amidpour M. Constructer design and optimization of a direct contact humidification–dehumidification desalination unit. Desalination 2012;293:69–77.
[20] Shatat M, Omer S, Gillott M, Riffat S. Theoretical simulation of small scale psychometric solar water desalination system in semi-arid region. Appl Therm Eng 2013;59:232–42.
[21] McGovern Ronan K, Gregory P, Thiel G, Narayan P, Zubair SM, John H, et al. Performance limits of zero and single extraction humidification–dehumidification desalination systems. Appl Energy 2013;102:1081–90.
[22] Shen J, Xing Z, Wang X, He Z. Analysis of a single-effect mechanical vapor compression desalination system using water injected twin screw compressors. Desalination 2014;333:146–53.
[23] Ben Halima H, Frikha N, Ben Slama R. Numerical investigation of a simple solar still coupled to a compression heat pump. Desalination 2014;337:60–6.
[24] Kang H, Yang Y, Chang Z, Zheng H, Duan Z. Performance of a two-stage multi-effect desalination system based on humidification–dehumidification process. Desalination 2014;344:339–49.
[25] Ghalavand Y, Hatamipour MS, Rahimi A. Humidification compression desalination. Desalination 2014;341:120–5.
[26] Aybar Hikmet S. Analysis of a mechanical vapor compression desalination system. Desalination 2002;142:181–6.
[27] Zhang LZ, Zhu DS, Deng XH, Hua B. Thermodynamic modeling of a novel air dehumidification system. Energy Build 2005;37:279–86.
[28] Bahar R, Hawlader MNA, Woei LS. Performance evaluation of a mechanical vapor compression desalination system. Desalination 2004;166:123–7.
[29] Ettouney H, El-Dessouky H, Al-Roumi Y. Analysis of mechanical vapor compression desalination process. Int J Energy Res 1999;23:431–51.
[30] Al-Enezi G, Ettouney H, Fawzy N. Low temperature humidification dehumidification desalination process. Energy Convers Manage 2006;47:470–84.
[31] Nafey AS, Mohamad MA, El-Helaby SO, Sharaf MA. Theoretical and experimental study of a small unit for solar desalination using flashing process. Energy Convers Manage 2007:48–538.
[32] Mohamed AMI, El-Minshawy NA. Theoretical investigation of solar humidification–dehumidification desalination system using parabolic trough concentrators. Energy Convers Manage 2011;52:3112–9.
[33] Ghazal MT, Atikol U, Egelioglu F. An experimental study of a solar humidifier for HDD systems. Energy Convers Manage 2014;82:250–8.
[34] Yıldırım C, Solmus I. A parametric study on a humidification–dehumidification (HDH) desalination unit powered by solar air and water heaters. Energy Convers Manage 2014;86:568–75.
[35] Fouda A, Melikyan Z. A simplified model for analysis of heat and mass transfer in a direct evaporative cooler. Appl Therm Eng 2011;31:932–6.
[36] (http://www.ahi-carrier.com.au/product.cfm?productid=46&content=52) [last accessed 26.11.2014].
[37] Yogesh J. Design and optimization of thermal systems. 2nd ed. CRC Press; 2007.